

SILICON-BASED FLAME RETARDANTS

by

**Takashi Kashiwagi and Jeffrey W. Gilman
Building and Fire Research Laboratory
National Institute of Standards and Technology
Gaithersburg, MD 20899 USA**

Reprinted from the Fire Retardancy of Polymeric Materials. Chapter 10, Marcel Dekker, Inc., New York, NY, Grand, A. F.; Wilkie, C. A., Editor(s), 353-389 p., 2000.

NOTE: This paper is a contribution of the National Institute of Standards and Technology and is not subject to copyright.



NIST

National Institute of Standards and Technology
Technology Administration, U.S. Department of Commerce

10

Silicon-Based Flame Retardants

Takashi Kashiwagi and Jeffrey W. Gilman

National Institute of Standards and Technology, Gaithersburg, Maryland

I. Introduction	353
II. Silicone	354
III. Silica	360
IV. Preceramic Polymer Blends: Silanes and Silsesquioxanes	367
V. Silicates	374
VI. Polymer Layered-Silicate (Clay) Nanocomposites	379
VII. Summary	386
References	387

I. INTRODUCTION

The number of new articles, patents, and products associated with silicon-based flame-retardant (FR) systems is evidence of renewed interest in FR approaches that do not rely completely on halogens or phosphorus (1–7). Almost all forms of silicon have been explored as flame retardants. This chapter will attempt to present excerpts from the various subtopics within the area of silicon-based flame retardants. This chapter is not an encyclopedic review of the literature associated with Si-based FR; instead, we have tried to show the FR behavior and mechanism for the most common Si-based approaches. The following silicon-based materials will be covered: silicones, silicas, organosilanes, silsesquioxanes, and silicates.

This is a publication of the National Institute of Standards and Technology (NIST), an agency of the U.S. government, and by statute is not subject to copyright in the United States.

We will address these materials when used in copolymers, polymer-polymer blends, and as additives.

II. SILICONE

The most common flame retardant based on silicon is in the form of polyorganosiloxane—in particular, polydimethylsiloxane (PDMS). A group at General Electric has worked extensively on block copolymers of various types of polycarbonates (8–12) and polyetherimides (13) with PDMS. The multisequence bisphenol fluorenonecarbonate PDMS block copolymers, BPFPC–PDMS, were synthesized with mass fraction of up to 27% silicone, and PDMS blocks with number-averaged degree of polymerization from 10 to 40 (8,9). Although both modulus and yield stress decreased with increasing silicone content, independent of block length, impact toughness and plane strain-stress intensity factors increased with silicone content. The limiting oxygen index (LOI) of these block copolymer samples shows significant increase from 38 to 40 for BPFPC alone, to as high as 51 (this is at a relatively low silicone level). In fact, LOI does not increase with silicone content above mass fractions of 15%, as shown in Fig. 1. Therefore, BPFPC resins, with mass fractions from 15% to 20% silicone, can have a balance of properties that makes them attractive as tough, transparent, flame-resistant engineering plastics.

This work extended up to a mass fraction of 62% PDMS content (with the degree of polymerization from 10 to 30) in the bisphenol fluorenes (BPF). Three blends of BPFPC homopolymer with BPFPC–PDMS block copolymer (PDMS mass fraction of 62%) were also formulated. Blends with three levels of PDMS resulted (total mass fraction of PDMS: 10%, 20%, and 30%). The results show that a maximum in LOI is reached at about a mass fraction of 8% silicon, as shown in Fig. 1 (11). The residue changed from a fine, black, friable char from the homopolymer, to a more voluminous, very strong, largely black char at moderate amounts of silicone, to a gray, coarse, weak residue at high silicone contents. By contrast, the SiO_2 -filled homopolymer burned slowly with little or no swelling of the residue. Additionally, other polycarbonates based on bisphenol A (BPAPC) and PDMS block copolymers were synthesized and tested. The LOI increased, reaching a broad maximum at 38–40 in this family with mass fractions of 15% to 30% PDMS. The LOI decreased at higher mass fractions of PDMS. No clear dependence of LOI on block length at fixed silicone content was observed. In contrast to BPFPC, BPAPC tends to drip somewhat on burning, so that the char that forms on the BPAPC homopolymer does not form a stable protective cap. The bisphenol chloral polycarbonate (BPCPC) block copolymer with PDMS shows a small increase in LOI at low silicone content (about a mass fraction of 10%), but no increase in LOI was observed for phenolphthalein polycarbonate with PDMS.

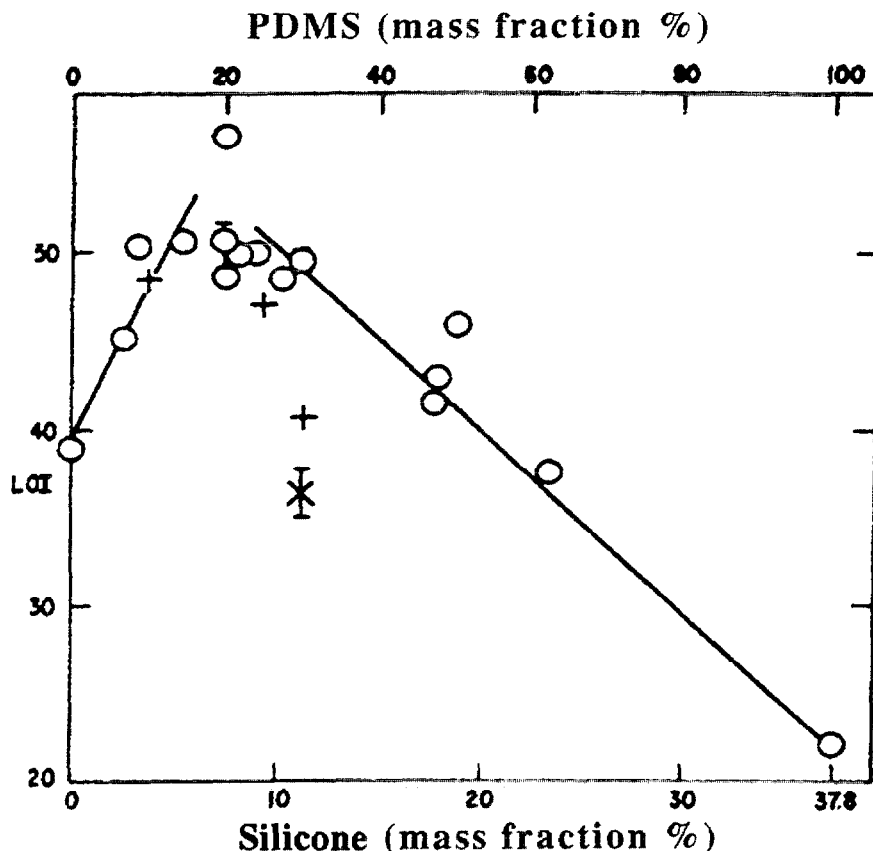


Figure 1 The effect of silicone content on LOI of BPFPC; (O) block copolymer, (+) pure BPFPC and block copolymer blend, (X) pure BPFPC and SiO₂ (upper PDMS scale applies for all materials except the SiO₂ mixture). (From Ref. 11.)

Polystyrene-silicone block copolymers show two different trends in LOI. The copolymer which exhibited little molten polymer flow during the test had a greater increase in LOI than the copolymer with significant molten polymer flow. Very little LOI enhancement was observed for high-molecular-weight poly(methyl methacrylate)-silicone block copolymers. All these results indicate that the conversion of an organic polymer to a mechanically stable char appears to be an important requirement to obtaining higher LOI values (11). Another study of block copolymers (14), polyurethane-PDMS showed that LOI increased nearly linearly with silicone content up to 50%, which is contrary to the trend of the initial increase followed by a decrease with silicone content, as shown in Fig. 1. This could be due to the low LOI for pure polyurethane (about 18) compared to 29 for pure PDMS. Thus, LOI of the polyurethane-PDMS tends to increase from 18 toward 29 with the increase in silicone content. However, the LOI of pure polycarbonates (about 30 for BPAPC and 40 for BPFPC) is relatively high compared to that of PDMS.

Analysis of degradation products by gas chromatography indicates that the peak in cyclic silicone evolution occurs at a temperature below that of the maximum BPFPC product evolution. The reduction in cyclic silicone evolution with increasing temperature occurs because of *in situ* oxidation, as evidenced by the white powder remaining at the end of the experiment. The particles in the residue appear to be amorphorous SiO_2 rather than SiO . The flame-retardant mechanism for PDMS in the block copolymers was initially postulated as follows: Cyclic silicone oxidation modifies a carbonaceous char that is a substantially continuous, stable, barrier impermeable to oxygen, which protects the underlying carbonaceous char from oxidative attack (9). However, the same author later suggested a different mechanism based on the chemical and physical characteristics of the char, not simply on measurements of char yield. He concluded that the increase in LOI for BPAPC-PDMS block copolymers results from an increase in the yield of the char, which is more resistant to oxidation from an improvement in the char as a transport (heat and mass) barrier (12). The improvement may stem principally from enhanced oxidation resistance arising from the silicon retained in the char and converted to a continuous protective silica layer during oxidation. This is the reason they offer for why their results show that van Krevelen's correlation between the char yield (even subtracting the accumulation of SiO_2 in the char) and LOI values (15) does not agree with their data. With non-char-forming polyurethanes, the addition of silicone blocks does not enhance the formation of carbonaceous char; their polymer residues are SiO_2 converted from organic silicones (14).

The flame-retardant effectiveness of silicones in all of the above studies was determined only by LOI and it would be more useful to measure their effectiveness in terms of more fire-relevant properties such as heat release rate and smoke yield. These properties were measured for polyetherimide-silicone block polymers in the Ohio State University (OSU) device for heat release rate (HRR) and in the NBS smoke chamber for smoke density (13). The results show that the peak HRR first decreases as silicone content increases, and then the peak HRR increases with further addition of silicone. The minimum peak HRR was obtained at a mass fractions of 5% PDMS. However, smoke density tended to increase with silicone content. Another study was made using BPAPC-PDMS (mass fractions of PDMS up to 5%) block copolymers in two calorimeters. One using the Cone Calorimeter (for small samples of 10 cm \times 10 cm \times 0.3 cm thick); the other using the furniture calorimeter (for two sample sizes of 40 cm \times 40 cm \times 0.3 cm and 60 cm \times 60 cm \times 0.3 cm). The later tests were done to obtain flame-spread rate measurements (16). The average HRR and peak HRR of the samples decreased with an increase in silicone content, but this decrease became smaller with increased silicone content. Above mass fractions of PDMS of 4%, the peak HRR did not change. The total heat release, which was obtained by integrating HRR over the total burning time, did not change significantly with silicone content. The piloted ignition time gradually decreased with increased silicone content, and soot yield did not change significantly with silicone content. Overall, the BPAPC-

PDMS block copolymers burned slowly but for a longer time than the homopolymers. The pure polycarbonate (PC) sample generated a brittle, thin shell-like char layer. The BPAPC–PDMS samples tended to generate a foamy, less brittle intumesced char mass. However, the intumesced char mass was formed behind the flame-spread front and, therefore, the char did not prevent or even slow down flame spread. Actually, the flame-spread rate over the BPAPC–PDMS sample surface was faster than that over the pure PC sample. This is consistent with the observed shorter piloted ignition delay time for the BPAPC–PDMS samples measured in the Cone Calorimeter, as the flame-spread process can be considered a series of successive piloted ignition phenomena.

Another approach is the incorporation of silicon into the branches of the polymer chains. This approach was applied to polystyrene (PS) and poly(vinyl alcohol) (PVA) by substituting hydrogen at the para position of the benzene ring in PS, and by substituting the hydrogen in the hydroxyl of PVA with a silane (17). Chlorosilanes and dichlorosilanes were also substituted at the same locations. The results show a significant increase in LOI with the addition of chlorine from chlorosilane or dichlorosilane to the branches, compared not only with the original polymers but also with brominated PS. Char yield, measured by thermogravimetric analysis (TGA), increases with more chlorine substitution, but the Si yield in the char decreases with the increase in chlorine content. It appears that silicon has a much greater effect in the presence of halogen. It is postulated that the evolution of silicon chlorides enhances flame suppression in the gas phase (18,19) and the high char yield reduces the amount of evolved combustible degradation products in these systems.

It appears that the flammability properties of polymer and silicone blends are about the same as those of polymer–silicone copolymers (16). Because the cost of the blends would be less than that of the copolymers, several silicone blends were examined as flame-retardant systems. However, their flame-retardant effectiveness is not sufficient and, generally, other flame-retardant additives such as a small quantity of halogenated additives or halides are used together with silicone additives to get a UL-94 V-0 rating (20–24). Three of the previous applications were for polypropylene (PP) (20–22) and the fourth study was for ethylene butyl acrylate (EBA) (23). The fifth study applied to various resins including PS, PP, PC, ethylene vinyl acetate (EVA), and others (24). Generally, the peak and average heat release rates of these samples with silicone additives are significantly reduced without increased smoke and CO yields, but the total heat release tends to be about the same as that of the pure resins. An example of the heat-release-rate curve is shown in Fig. 2 for PS. It was also found that the addition of silicone with halogenated flame retardants reduces further the heat release rate and, furthermore, improves some of the physical properties that are reduced by the addition of the halogenated flame retardants alone (24). It was postulated that the combination of polysiloxane with chalk in EBA enhances the formation of char. Using energy-dispersive x-ray spectroscopic analysis and infrared analysis, the main

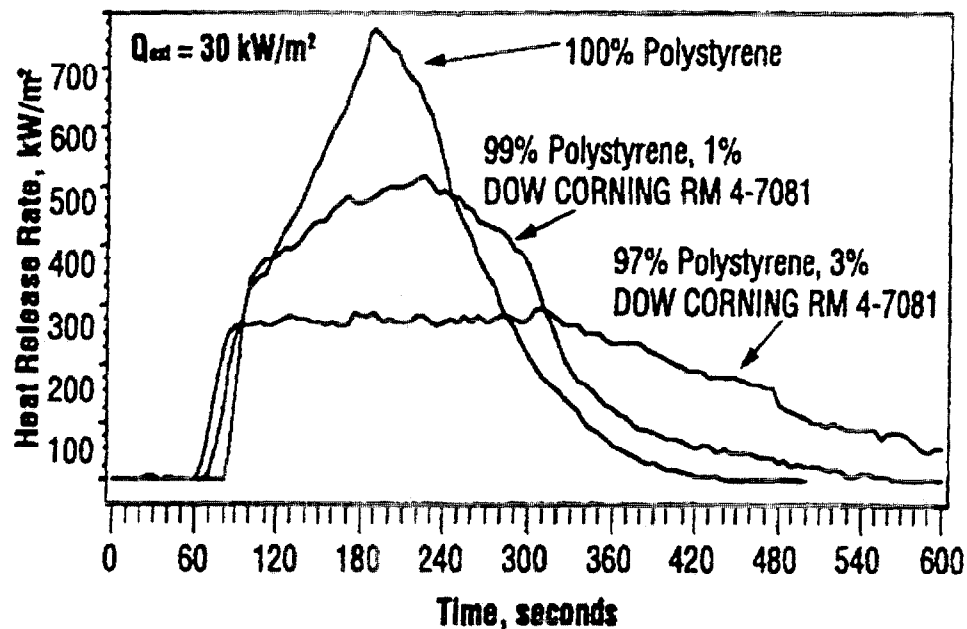


Figure 2 The effect of the silicone-based additive on the heat release rate of PS. (From Ref. 24.)

component of the burned residue in the Cone Calorimeter was found to be calcium carbonate, with a minor component being silica (23). Another interesting study is the synergistic flame-retardant behavior of silicone gum with lead phthalate in polyethylene (PE) (25). Initially, the authors of this study intended to form a lead silicate glass, but examination of residues showed no evidence of glass formation. Their careful study indicates that the lead-silicone system is a solid-phase flame retardant. This is supported by the analysis of the residues using both an energy-dispersive x-ray technique with a scanning electron microscope and Electron Spectroscopy for Chemical Analysis (ESCA). The results indicated that lead was present as metal and as the oxide. It was postulated that cross-linking is crucial in allowing the reaction between lead and silicone to form the slow-burning, foamed caducous char that is necessary to afford a flame-resistant material (25). One case of silicone blend was intended to be used as a surfactant for flexible polyurethane with flame-retardant systems. However, the use of an appropriate chemical structure of the siloxane component resulted in less use of the flame-retardant systems to meet the ASTM 1692 burn test requirement (26,27).

All of the above silicone additives for PP and PE did not get a UL-94 V-0 rating without additional flame-retardant additives. However, recently, a specific silicone addition to PC achieved V-0 rating with less than 10% by mass (7). Although the flammability properties of PC are better than those of PP, this is one of the rare cases in which a relatively small quantity of a silicone additive achieves a V-0 rating without any additional additives. This particular silicone additive is tai-

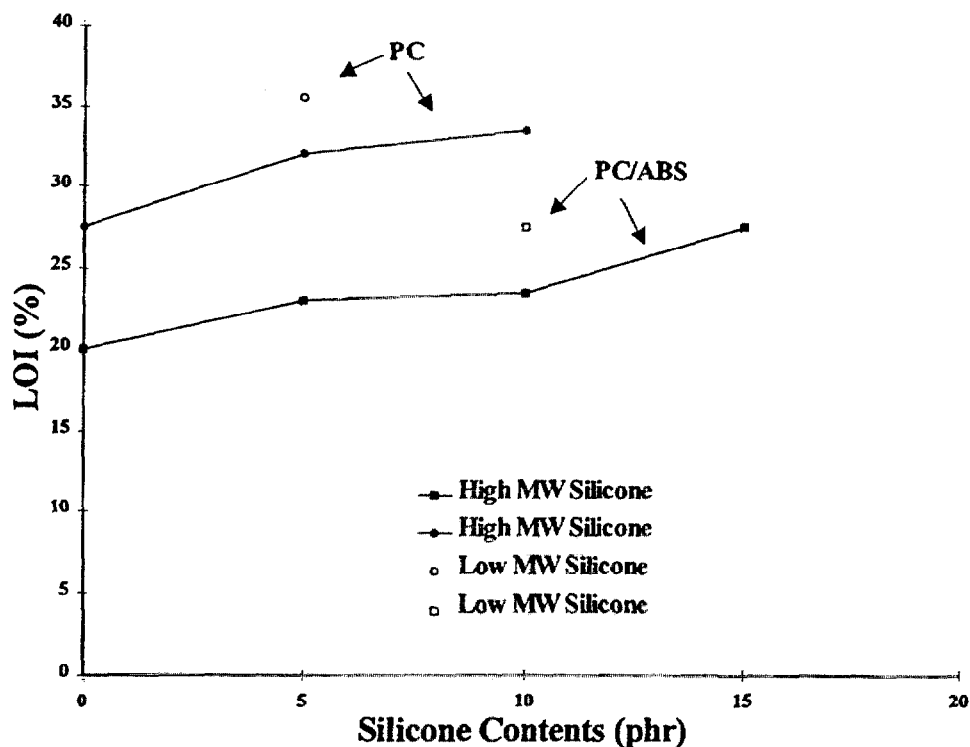


Figure 3 The effect of silicone content on LOI. (From Ref. 7.)

lored to be compatible with PC and also to PC-acrylonitrile-butadiene-styrene (ABS) so as to maintain the physical properties of the original resins. The relationship between LOI and silicone additive content for this system is shown in Fig. 3. Its chemical structure is shown in Fig. 4. Because it contains aromatic components in its structure, its dispersity in the resins is much better than dimethyl-silicones. The impact strength of PC with the silicone is nearly the same as that of PC alone. The ratio of Si to C in a burned sample measured by x-ray photoelec-

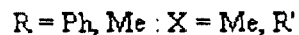
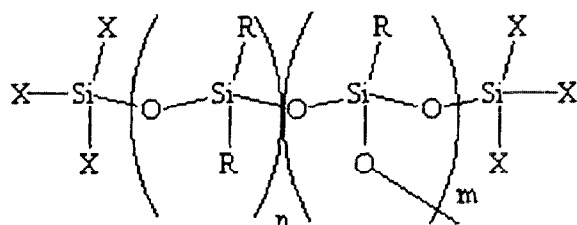


Figure 4 Chemical structure of a new silicone-based flame-retardant additive. (From Ref. 7.)

tron spectroscopy (XPS) is much higher than that of the original sample and its flame-retardant mechanism is postulated to be by the formation of a protective surface layer consisting of the combination of silicon and carbonaceous char (7). This application raises the possibility of utilizing more effective flame-retardant silicone additives than the traditional dimethylsiloxane-based additives and their potential to be used over a wide range of applications because of the advantage of their environmentally friendly nature.

III. SILICA

Inorganic silicon-based additives such as silica have been used as a filler instead of as a flame retardant, but under certain cases, the addition of silica affects the thermal stability of PP, depending on the active metal content such as Ti, Al, and Fe in the silica (28); it also affects the flammability properties of materials (29–31). It was found that silica was needed as a filler for a small quantity of platinum to become effective to increase in LOI for a peroxide-cured silicone rubber (29). The effects of the amount of filler on LOI with and without platinum are shown in Fig. 5. 2,4-Dichlorobenzoyl peroxide was used to cross-link the silicones to rubber, but the addition of the peroxide significantly reduced the LOI without the silica and platinum. These results show that LOI decreases with an increase in cross-link density as measured by swelling. It is generally demonstrated that cross-links improve flammability as observed in another study by the same author (25). However, the author postulates that initial cross-linking onto the silica surface is detrimental to producing a flame-retardant rubber. This conclusion was derived from the result in which a higher LOI was demonstrated using silanol-treated silica (lower cross-link density). The decrease in LOI with an increase in cross-link density could be due to the reduction in mobility of cross-linked silicones to the burning surface to form a protective layer (7). Another explanation could be that the observed sharp drop in LOI with curing by the peroxide might be caused by a small quantity of unreacted peroxide (this could be further supported by the fact that LOI does not change significantly with the change in peroxide concentration from 0.4% to 2.6% for the case without platinum and silica). The thermal stability of silicones at high temperatures is extremely sensitive to impurities such as a minute quantity of the residual catalyst used for polymerization (32). In this case, the effects of cross-links on LOI might be a secondary factor.

The effects of the type of filler between hydrated silica versus hydrated alumina on the flammability of the intumescent system PP with ammonium polyphosphate (APP) were studied by various flammability indices measurements, including LOI (30). The results show that there are no significant differences in

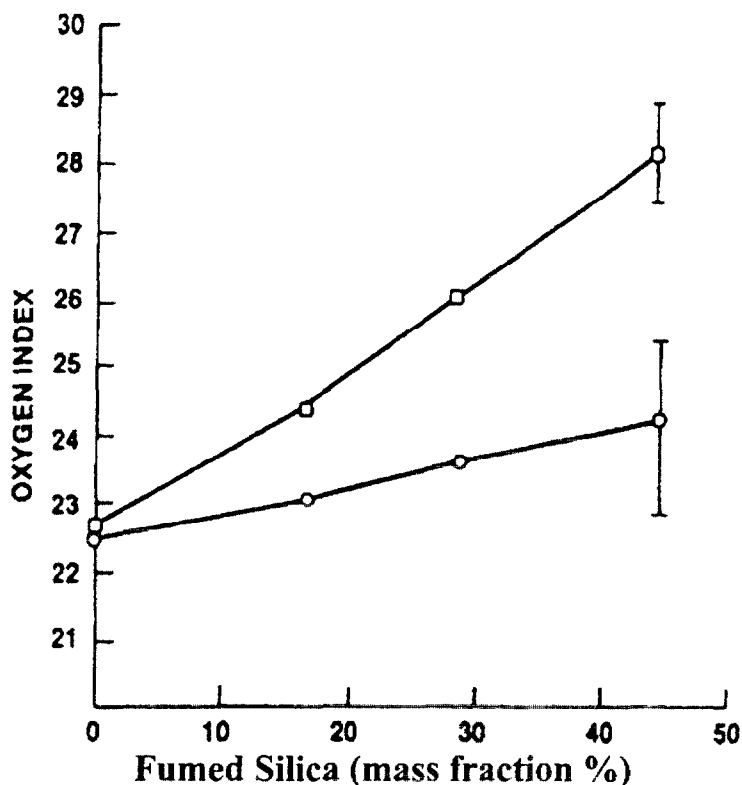


Figure 5 The effect of filler (fumed silica) on LOI. ○: No platinum; □: 60 ppm platinum. (From Ref. 30.)

flame-retardant effectiveness between the two fillers and all indices are decreased more than 5% by both fillers due to a decrease in intumesced char height by the gradual collapse of cellularlike char structure. It appears that the intumesced char height tends to be less with silica hydrate than with aluminum hydrate, but thermal insulating performance for the char formed with silicate hydrate is better than that formed with aluminum hydrate. Another modifier of the PP-APP intumescent system is boron-siloxane, which is more stable against water and tends to improve the LOI due to the migration of the boron-siloxane elastomer to the surface (31). However, these two silicon-based additives are not primary flame-retardant additives; they are used to further improve the flame-retardant effectiveness of the primary APP system.

Systems involving a combination of silicon with tin chloride (18,19) and silica itself (33,34) were used as primary flame-retardant additives to various commodity polymers. In the former study, it was determined that a small amount of silicon with tin chloride (3 mass% and 2 mass%, each) increased the ignition delay time and the reduced heat release rate simultaneously and also decreased the total heat release rate. Such a flame-retardant performance is generally not

achieved by silicon/silicone-based additives, as described earlier. Although about 10 mass% of residue was left at the end of tests in the Cone Calorimeter, it was postulated that the main flame-retardant mechanism is based on the gas-phase inhibition by SiCl_4 and HCl , which are by-products of a proposed reaction between silicon and tin chloride and also from the reaction of silicon tetrachloride with water. The mechanism by which the halosilane achieves flame inhibition is similar, if not identical, to the well-known halogenated, carbon-based retardants. This silicon-based flame-retardant approach is quite different from any of the above-cited approaches in which, generally, the silicon/silicone-based flame-retardant site is in the condensed phase. More conventional approaches to the intended flame-retardant activity in the condensed phase were used for cellulose (33) and various commodity polymers (34). The former study is based on a series of cellulose-polysilicic acid hybrid fibers with 15–35% silica content. The LOI of the hybrid fiber was substantially higher than that of comparable synthetic fibers and of cotton; the heat release rate was significantly lower, as was burning duration. It is postulated that flame retardancy is achieved by increasing the formation of a non-volatile residue.

The latter study (34) was motivated by a desire to obtain *in situ* formation of silicon-based flame retardants during combustion. The reaction of silica gel and organic alcohols in the presence of metal hydroxides has been shown to generate multicoordinate organosiliconate compounds (35). It was anticipated that a silicon-oxy-carbide protective char could be formed by combining a polyhydroxylic polymer such as poly(vinyl alcohol) (PVA) or cellulose, with silica gel and K_2CO_3 in the condensed phase of the pyrolyzing polymer surface during combustion. However, ^{29}Si -nuclear magnetic resonance (NMR) analysis of the char generated from combustion of PVA with silica gel- K_2CO_3 in the Cone Calorimeter indicates that the majority of the silica gel's original structure remained intact during the combustion and the envisioned silicon-oxy-carbide bonds were not observed. It appears that the temperature range for pyrolyzing polymers, from 300°C to 400°C, is too low to form such bonds (36). However, a significant reduction in heat release rate is observed with silica gel- K_2CO_3 (6 mass%/4 mass%) not only for polyhydroxylic polymers but also for nonhydroxylic polymers such as PP, PS, nylon 6,6, and poly(methyl methacrylate) (PMMA) (34). The ignition delay time and total heat release are not significantly affected by the addition of silica gel- K_2CO_3 . These trends are common to the above-described silicon/silicone-based flame-retardant approaches.

At present, it is not clear what mechanism is responsible for the significant reduction in heat release rate and for the enhancement in the formation of carbonaceous char for some of the polymers. In an effort to understand the mechanism, PMMA with silica gel and K_2CO_3 was studied further. This system forms carbonaceous char during combustion (34). Measurements were made of mass loss and mass loss rates in nitrogen at an external radiant flux of 41 kW/m^2 for

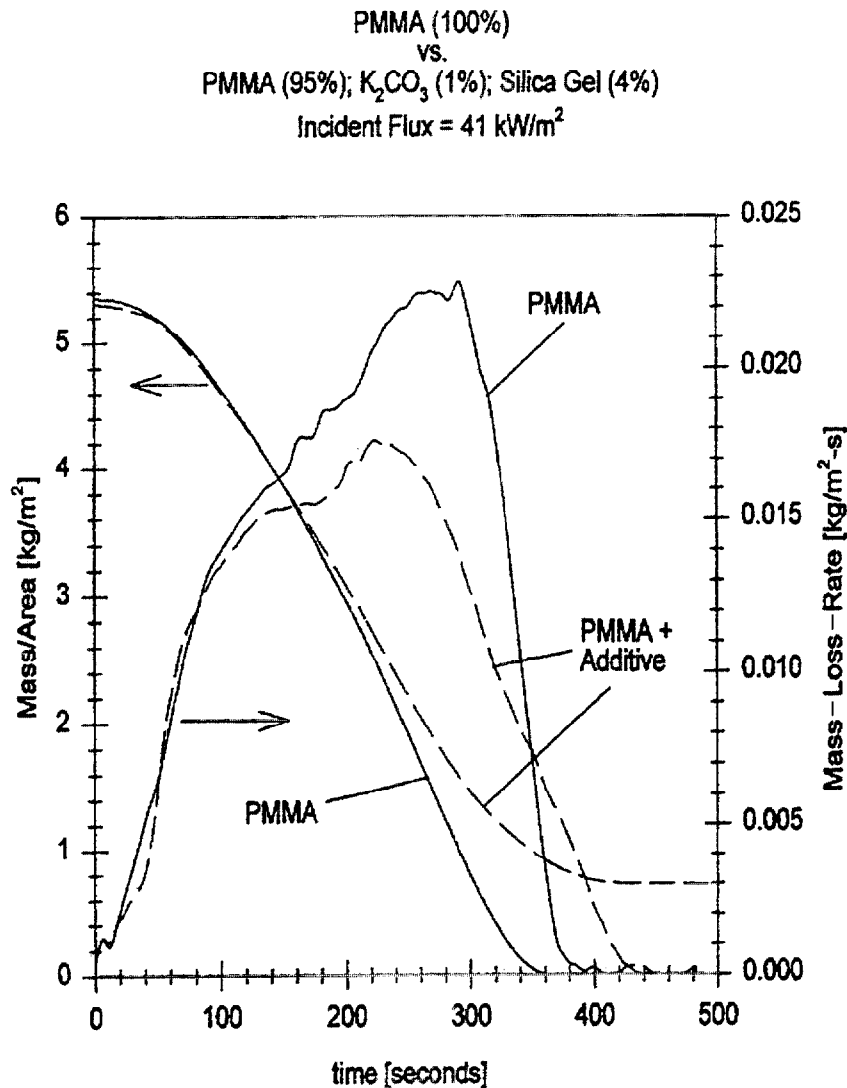


Figure 6 Mass loss and mass-loss-rate curves for PMMA and PMMA with silica gel-K₂CO₃ in nitrogen. (From Ref. 34.)

both pure PMMA and for PMMA with silica gel-K₂CO₃ (mass ratio: 95:4:1). Because there is no gas-phase reaction involved due to the pure nitrogen environment, the observed results are based solely on the chemical and physical processes in the condensed phase. The external thermal radiation is used to simulate the heat feedback from flames in a fire. A detailed description of the radiative gasification apparatus used in this study can be found in Ref. 34. The results are shown in Fig. 6. The mass loss rate up to about 100 s after the start of the radiant exposure is about the same for both samples, but beyond 100 s, the mass loss rate of PMMA

with silica gel- K_2CO_3 is about 20–25% less than that of PMMA. In the Cone Calorimeter, there are two energy fluxes to the sample surface; one is the radiative energy flux from a Cone heater and the other is the energy feedback from a flame. Because a lower mass loss rate (supply rate of combustible evolved products) tends to generate a smaller flame, it would reduce the energy feedback rate from the smaller flame to the sample surface. Therefore, the total energy flux to PMMA with silica gel- K_2CO_3 in the Cone Calorimeter is expected to be less than that of pure PMMA. (The results shown in Fig. 6 were based on the same external flux.) Therefore, it is expected that the reduction in heat release rate for PMMA with silica gel- K_2CO_3 would be close to 40%, which is the level observed in the Cone Calorimeter (34).

Digitized images of the video of both samples during a radiative gasification experiment in nitrogen, shown in Fig. 7, reveal that the PMMA sample does not form any carbonaceous char, but the PMMA with silica gel- K_2CO_3 sample becomes a dark color, showing the formation of carbonaceous char by 140 s. The formation of carbonaceous char continues, and roughly 15% of the original weight of the sample remains at the end of the experiment. A thermocouple embedded in the top surface of the sample showed that the temperature was 360–440°C at the time char began to form (~80 s). These data show that the silica gel- K_2CO_3 additives do not affect charring of the PMMA early in the degradation process until the temperature reaches about 360°C. However, the chemical reactions responsible for the formation of carbonaceous are not known at present.

A similar nitrogen gasification study was conducted with PP blended with three different types of silica gel: a large internal pore volume silica gel, a fused silica gel (no pore volume), and fumed silica with silanol capped (hydrophobic silica). All samples were made by compression molding. The comparison of mass loss rate in nitrogen between PP and PP with the three different types of silica gels is shown in Fig. 8. Although the mass loss rate of the PP with the silica gel was initially slightly higher than that of pure PP, it became significantly less than the latter beyond about 220 s. Up to 220 s, the visual appearance of the irradiated sample surface was about the same for all samples with significant melting and some bubbling. However, at about 220 s, the surface of the PP with the silica gel rapidly solidified and a crustlike layer was formed. It appeared that this layer continued to become thicker with time; the production of the evolved degradation products slowed down significantly. The layer appears to act as a thermal insulator and also act as a barrier to evolved degradation products. A preliminary study showed that the measured silicon mass concentration at the surface of the residue by the end of the test (using neutron activation analysis) was roughly 10 times larger than that from the initial value. A similar increase in silicon concentration during the test was also found in a previous study (7). Carbonaceous char is not

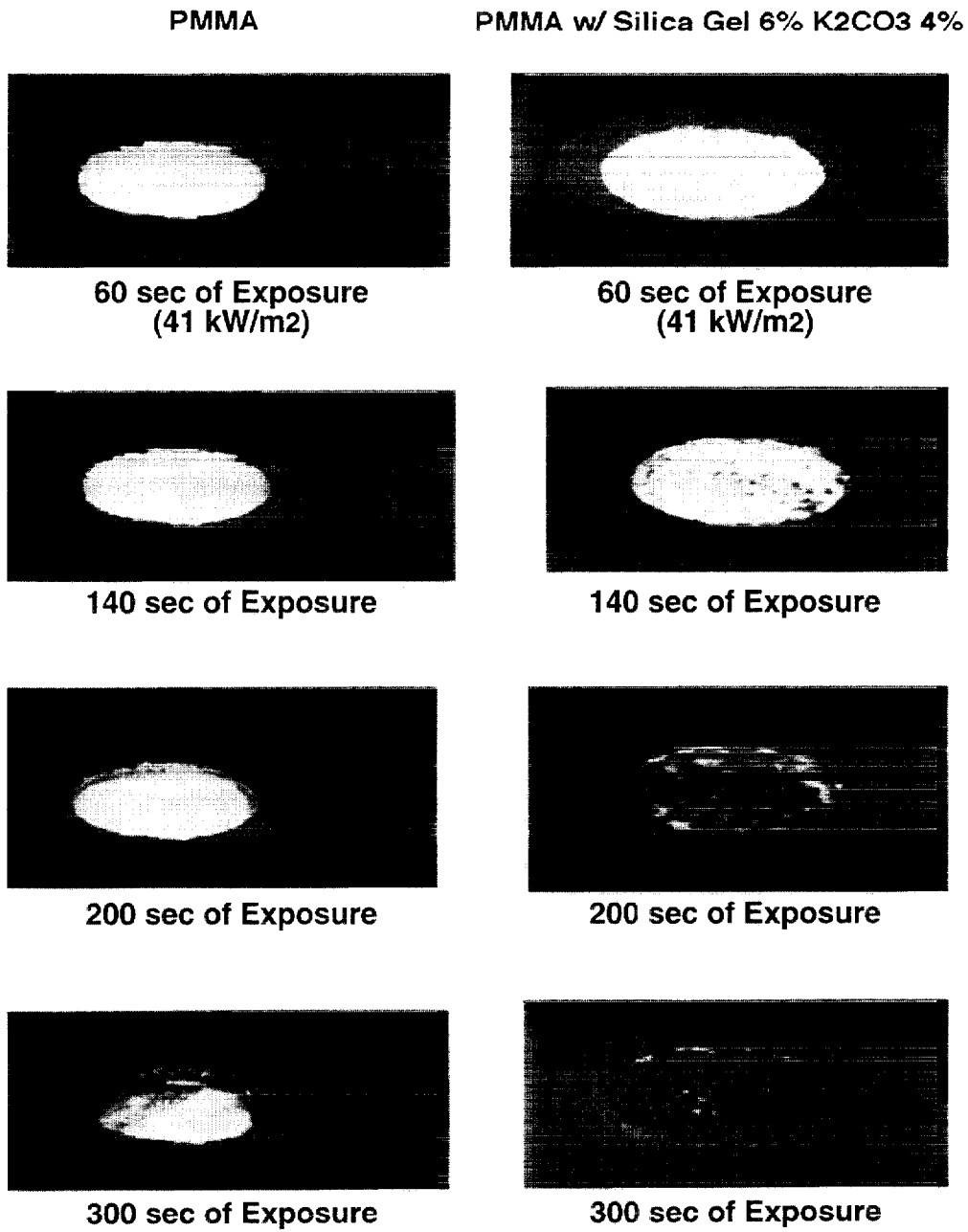


Figure 7 Video images of gasification experiments for PMMA and PMMA with silica gel-K₂CO₃ (95:4:1) in nitrogen at an external flux of 41 kW/m². (From Ref. 34.)

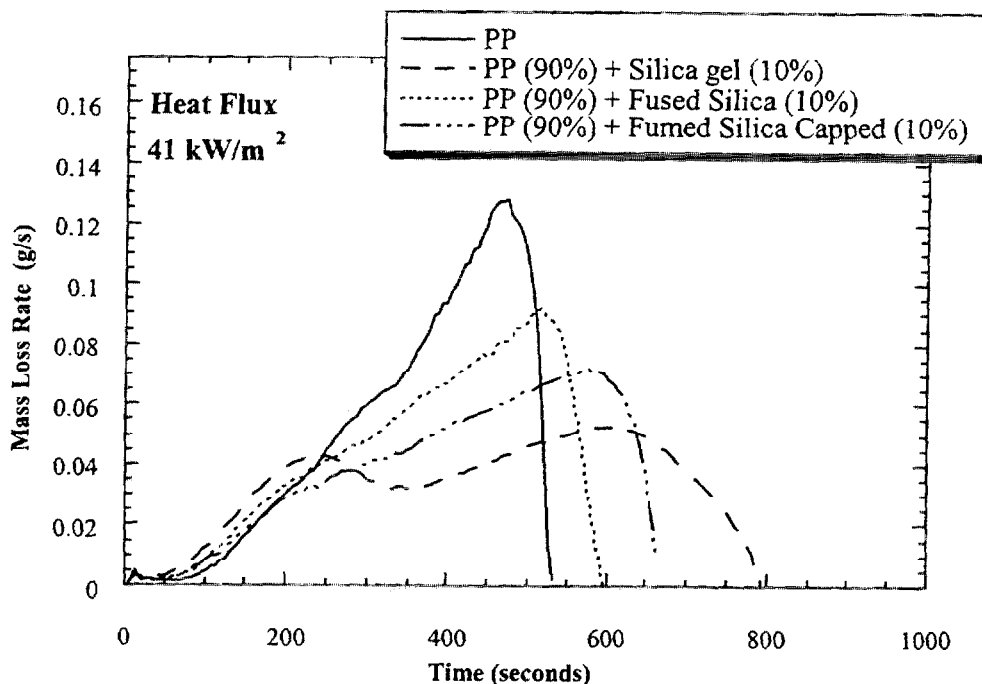


Figure 8 The effect of different types of silica gel on the mass loss rate of PP during gasification experiments in nitrogen.

formed for PP with silica gel or any of the silicas. The measured silicon mass concentration in the residue top layer by neutron activation analysis and Fourier-transform infrared (FTIR) analysis of the residue indicated that the majority of the residue top layer consisted of SiO_2 . However, the residue from PP with silica gel appeared to be a rigid crust instead of powders. The formation of the crust layer was not observed with the fused silica without pores (however, vigorous bubbling and the formation of a thin foam layer consisting numerous small bubbles of PP were toned down with the fused silica) and its effects on mass loss rate were much less than that for PP with the silica gel having a large pore volume, as shown in Fig. 8. The residue with the fused silica after the test was powdery instead of a rigid crust. The rigid crust was not formed for PP with the hydrophobic fumed silica. However, the vigorous bubbling observed for PP was significantly suppressed and large size bubbles were formed in the more viscous polymer melt layer. The mass loss rate of PP with hydrophilic fumed silica (not shown in Fig. 8) is almost exactly the same as that of PP with silica gel. Although it did not form the crust layer, it formed a fluffy white silica surface layer at the end of the test. It appears that two important parameters of silica characteristics for the reduction in mass loss rate of PP (also as effective flame retardants), which are silanol concentration

and a pore volume. However, these characteristics tend to be physical flame-retardant processes instead of chemical processes. The physical processes of the flame-retardant mechanism of the addition of silica in PP consist of two mechanisms; one is reduction in the transport rate of the thermal degradation products and the other is reduction in thermal diffusivity of the sample near the surface due to gradual accumulation of silica, which acts as a gradually thermal insulation layer. The reduction in the transport rate of the degradation products is achieved by dramatically increasing the viscosity of PP melts (nonpolar fluids) due to hydrogen-bonding of hydroxyl groups of silanol and entangling of polymer chains with the large pores of silica. The transport process mechanism tends to dominate early in the test because a small amount of silanol increases the melt viscosity dramatically (37,38), but the insulation mechanism requires a relatively large accumulation of fumed silica or silica gel for the accumulated layer to become an effective insulation layer.

The above discussion indicates that the formation of a silicon-based protective surface layer (39) appears to be the flame-retardant mechanism for silicone and silica systems. The combination of tin chloride and silicon appears to act in the gas phase (18,19). However, the pyrolysis temperatures of polymers are generally too low to form a glasslike protective surface layer. The silicon-based additives by themselves generally do not enhance the formation of carbonaceous char, except, possibly, the additive with a different silicone structure (7). The silica and dimethylsiloxane-based flame-retardant approaches tend to act in the condensed phase by a physical flame-retardant mechanism rather than a chemical one.

IV. PRECERAMIC POLYMER BLENDS: SILANES AND SILSESQUIOXANES

Work reported by several different groups illustrates the effectiveness of using Si-based polymers as flame retardants; either in blends, coatings, copolymers, or as the matrix for composites. The most common Si-based FR approach, using polydimethylsiloxane in blends and copolymers, has been investigated by many groups and is discussed in detail in Section II. Gilman et al. (40,41) have reported on the use of Si-based preceramic polymers as flame retardants in blends with thermoplastic polymers. Kowbel et al. have demonstrated the use of preceramic polymers as FR coatings on phenolic fabrics (42), and Chao et al. have prepared silsesquioxane-silicone resin composites, which showed very low flammability, typical for these resins (43).

Here, we will focus on the flammability of blends of preceramic polymers with thermoplastic polymers, due to the broader applicability of a blends ap-

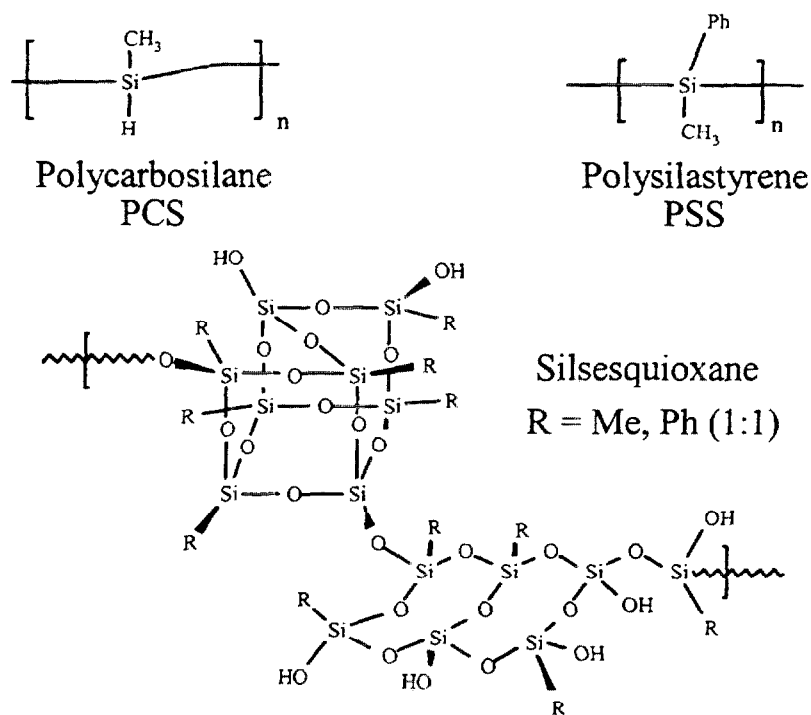


Figure 9 PCS, PSS, and polysilsesquioxane structures.

proach. Figure 9 illustrates the polycarbosilane (PCS), polysilastyrene (PSS), and polysilsesquioxane preceramic polymers which were blended with various thermoplastics, such as SBS (polystyrene–polybutadiene–polystyrene) and PTME–PA (polytetramethylenylether–glycol-*b*-polyamide-12, 1% polyamide-12) and polypropylene.

Compositions for the PTME–PA/PCS and PTME–PA/PSS blends, ranging from 20/80 to 80/20 (mass ratio) were prepared via solution blending in tetrahydrofuran (THF). Blends of SBS/silsesquioxane, SBS/PCS and PTME–PA/silsesquioxane were also prepared via solution blending in THF. The mechanical and thermal properties were investigated along with the flammability properties. Table 1 contains a partial listing of the thermal and mechanical properties for PCS, PSS, silsesquioxane, and the PTME–PA/PCS and PTME–PA/PSS blends (44).

Several overall trends are apparent from the data shown in Table 1. For example, as the amount of preceramic polymer in these compositions increases, so does the modulus of the resulting blend. In all cases, the modulus of the blend is higher than that for pure PTME–PA. This is roughly consistent with that expected for the mixing of a high-modulus material with a low-modulus one. In addition, as the relative amount of preceramic in these blends increases, the amount of ce-

Table 1 Properties for PCS, PSS, Silsesquioxane, and PTME-PA/PCS and PTME-PA/PSS Blends

Material	T_m (°C)	Char yield (%) ^a	Young's modulus (psi)
PTME-PA/PCS			
80/20	118	18 (17)	1,894
50/50	125	44 (38)	8,333
30/70	216	56 (53)	47,850
20/80	200	69 (59)	—
PTME-PA/PSS			
80/20	118	15 (18)	745
50/50	110	43 (41)	2,253
30/70	73	43 (56)	5,021
20/80	52	50 (63)	15,530
PTME-PA	119	2	581
PCS	199	74	—
PSS	148	79	—
Silsesquioxane (Me, Ph)	125	82	—

Note: Uncertainties: $\pm 5\%$ for T_m and char yields; $\pm 15\%$ for Young's modulus.

^aNumbers in italics represent calculated values (fraction of preceramic \times observed char yield for pure preceramic).

ramic produced (ceramic yield or char yield) upon pyrolysis is also observed to increase (see Fig. 10).

The char yields for the PTME-PA/PCS blends do not appear to be significantly increased by any interactions between the decomposition of the preceramic and that of the PTME-PA; that is, no significant additional carbon from the PTME-PA is retained in the ceramic char. This is also the case for the PTME-PA/PSS blends. However, the PTME-PA/PSS blends, containing mass fractions of 70% and 80% PSS, actually show a *lower* char yield than the theoretical or calculated yield (see Fig. 10). The char yields for these blends appears to level off at 45–50%.

Scanning electron microscopy (SEM) was used to examine the morphology of the blends. The PTME-PA/PCS compositions in Table 1 were found to be phase separated with 5–10- μ domain dimensions (see Fig. 11). The inhomogeneous character of these materials may result from insufficient mixing. However, it is most likely that the nonlinear, partially cross-linked structure of PCS and the insolubility of PTME-PA in the blending solvent (THF) contributed to the inhomogeneous character of the blend. Phase separation was not observed by SEM for any of the PTME-PA/PSS compositions. In addition, although the chemical

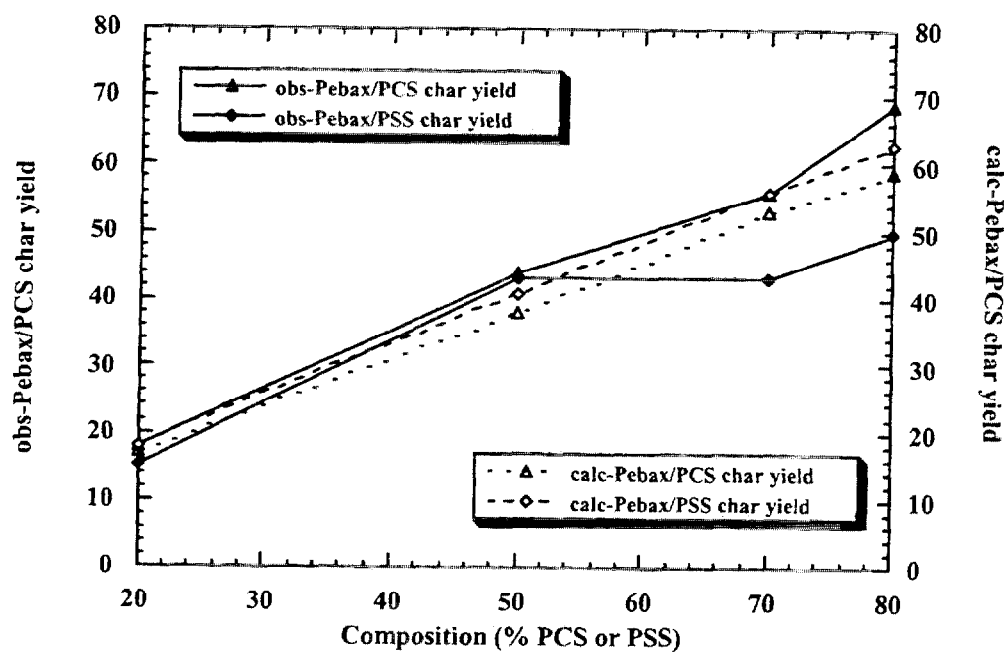


Figure 10 Plot of observed (obs) and calculated (calc) char yields for PTME-PA/PCS and PTME-PA/PSS blends at various blend compositions. Observed char yields were done via TGA (10°C/min, to 1000°C, N₂). The uncertainty is $\pm 5\%$ for char yields.

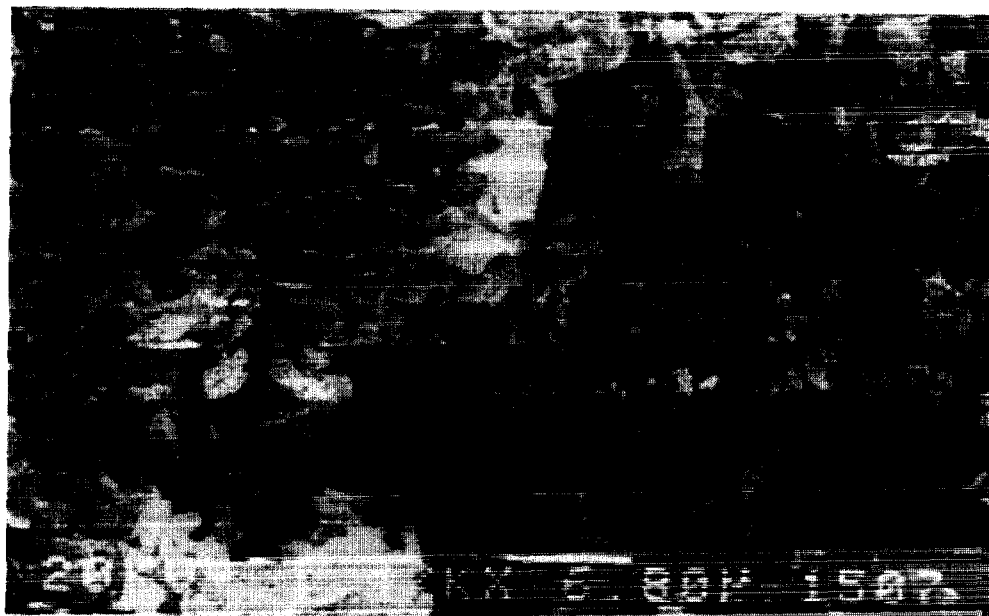


Figure 11 SEM of PTME-PA/PCS blend (mass fraction 50/50).

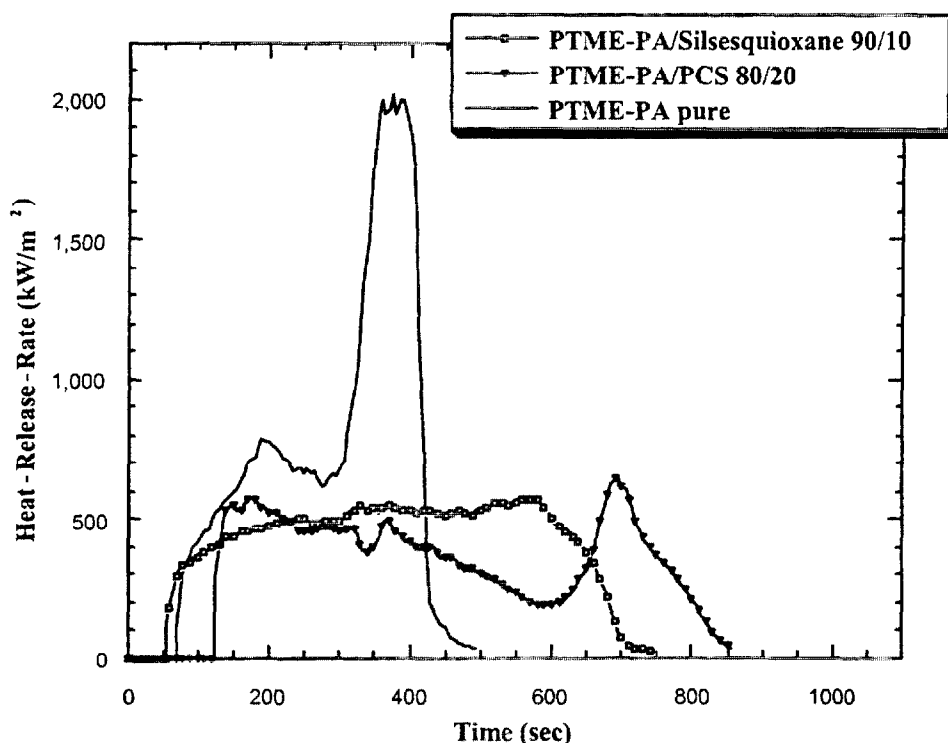


Figure 12 Heat-release-rate data for PTME-PA, PTME-PA/silsesquioxane 90/10 and PTME-PA/PCS 80/20. These data show a 60–70% reduction in the peak HRR and a 45% reduction in the average HRR for the blends.

structure of PCS and PSS are somewhat different, the linear polymeric structure of the PSS undoubtedly facilitated the blending of the PSS with the THF-swollen PTME-PA.

Due to the limitations of the PTME-PA/PSS blends (lower pyrolysis char yields at high preceramic fractions), flammability studies focused on the PTME-PA/PCS, SBS/PCS, PTME-PA/silsesquioxane, and SBS/silsesquioxane blends.

The flammability properties of these blends were characterized using the Cone Calorimeter (45). Samples were exposed to a 35-kW/m² heat flux. The results, shown in Figs. 12 and 13 and Table 2, reveal that both PCS and silsesquioxane are effective flame retardants. The HRR was reduced for the PTME-PA and SBS blends. An additional blend of silsesquioxane and PP also showed improved flammability performance. This was all accomplished at relatively low levels of incorporation of preceramic.

Although the preceramic polymers reduced the peak HRR and average HRR in both blends, the total HRR remained unchanged following combustion in the Cone Calorimeter. Furthermore, the char yields are about the same as the calcu-

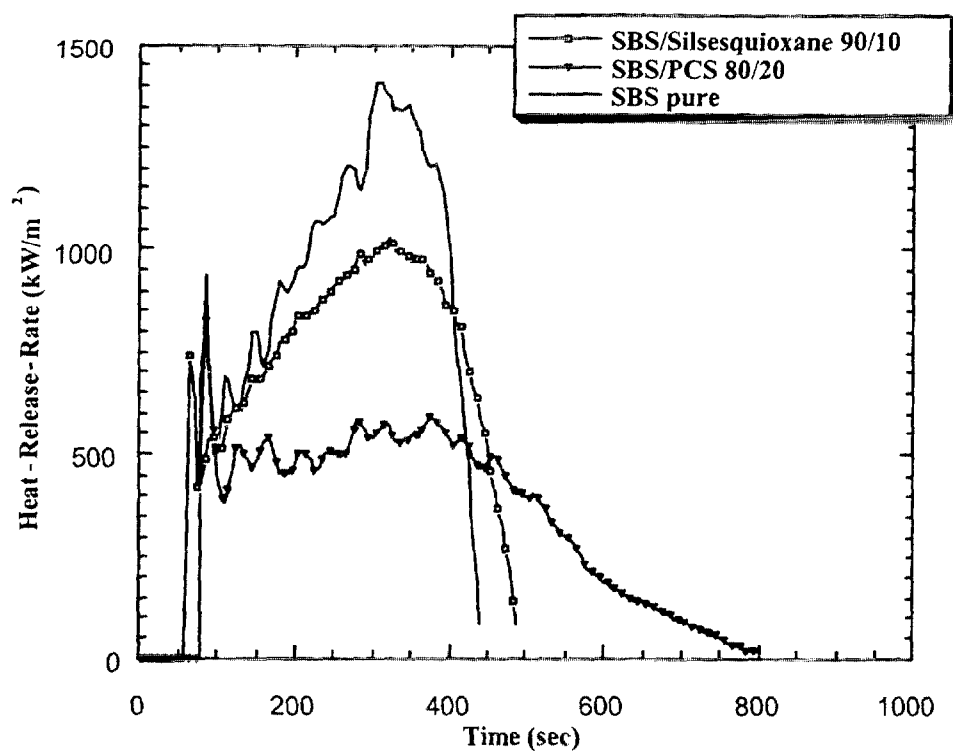


Figure 13 Heat-release-rate data for SBS, SBS/PCS (80/20), and SBS/silsesquioxane (90/10) blends. These data show a 30–40% reduction in peak HRR and a 20–60% reduction in average HRR for the blends.

lated yields (see Table 2, calculated yields are in parentheses). The addition of the preceramic polymers in these blends does not significantly increase the yield of carbonaceous char. This is the same result as that obtained in the char yields obtained in the TGA for PTME-PA/PCS blends, shown in Fig. 10. However, the mass-loss-rate data from the Cone Calorimeter, shown in Table 2, reveals that the primary reason for the lower HRR for the blends is the reduced mass loss rate; that is, the rate at which fuel is released into the gas phase is slowed by the presence of the ceramic char. Furthermore, because the heat of combustion, H_c , carbon monoxide yield, and specific extinction area (SEA) (measurement of smoke density) are not significantly different from those of the pure polymers, the preceramics do not affect the gas-phase combustion processes.

This means that the reduction in flammability is due to the protecting effect of the residue formed during the burning process, not from retention of carbon (fuel) in the condensed phase. Confirmation of the formation of ceramic-like residue comes from solid-state ^{13}C -NMR analysis of the residue from combustion of SBS/PCS, as shown in Fig. 14. Although, there are limitations on deriving quantitative information about combustion residues using only CP/MAS

Table 2 Cone Data for PTME-PA, SBS, and PP Combined with PCS and Silsesquioxane Preceramics

Sample	Char yield (%)	Mean mass loss rate (g/s m ²)	Peak HRR ($\Delta\%$) (kW/m ²)	Mean HRR ($\Delta\%$) (kW/m ²)	H_c^a (MJ/kg)	SEA ^b (m ² /kg)	Mean CO yield (kg/kg)
PP	0	25.4	1466	741	34.7	650	0.03
PP/ silsesquioxane 80/20	17 (16)	19.1	892 (40%)	432 (42%)	29.8	820	0.03
PTME-PA	0	34.2	2020	780	29.0	190	0.02
PTME-PA/ PCS 80/20	15 (15)	14.8	699 (65%)	419 (46%)	28.5	260	0.02
PTME-PA/ silsesquioxane 90/10	6 (8)	19.8	578 (72%)	437 (44%)	25.2	370	0.02
SBS	1	36.2	1405	976	29.3	1750	0.08
SBS/PCS 80/20	20 (15)	18.5	825 (42%)	362 (63%)	26.4	1550	0.07
SBS/ silsesquioxane 90/10	6 (8)	31.2	1027 (27%)	755 (23%)	26.9	1490	0.07

Note: Uncertainties: $\pm 5\%$ of reported value for char yields, HRR, and H_c data; $\pm 10\%$ for the carbon monoxide and SEA data. Theoretical char yields are in parentheses.

^aMean heat of combustion.

^bSEA = Specific extinction area (smoke measurement).

¹³C-NMR (due to unpaired electrons and low concentrations of protons) (46) qualitative conclusions can be drawn from the spectra shown in Fig. 14, especially using the protonated carbon spectrum shown at the top of Fig. 13. The spectrum indicates, qualitatively, that the SBS/PCS-char structure is dominated by carbon bonded to silicon (40 ppm to -10 ppm) as in amorphous silicon carbide (47). It appears that some amount of the char is aromatic-olefinic carbon (160-120 ppm).

In the PTME-PA blends, the silsesquioxane preceramic was more effective than the PCS preceramic at reducing the HRR. Only half as much silsesquioxane was needed to give a greater reduction in peak HRR and a comparable reduction in average HRR, as compared to the results for the PCS. This was not the case for the blends with SBS. In the SBS blends, the PCS functioned as well as in the PTME-PA blends. The silsesquioxane, however, performed less effectively in the SBS blends, even if the lower loading level is taken into account. The origin of the differences in performance for the two preceramics is under investigation.

This approach to flame-retarding commodity polymers is promising, be-

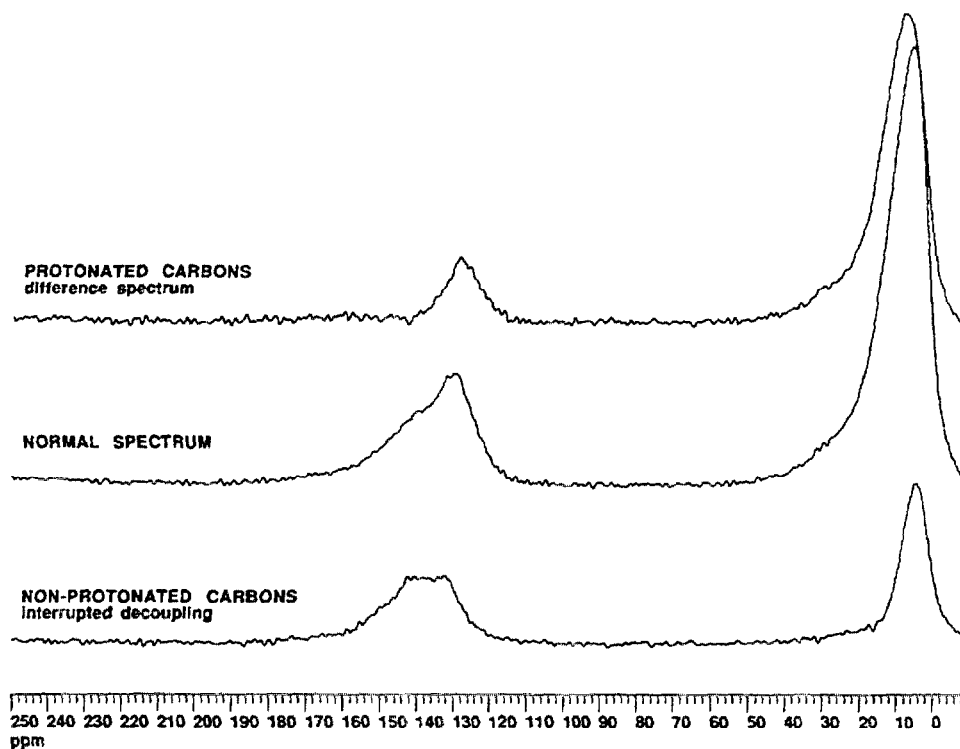


Figure 14 Solid-state ^{13}C -NMR (CP/MAS) spectra of SBS/PCS (80/20 mass ratio) char. The middle spectrum (normal CP/MAS) shows aromatic-olefinic carbon from 160 ppm to 110 ppm, aliphatic carbon from 40 ppm to 10 ppm, and carbon near silicon from 40 ppm to -10 ppm. The bottom spectrum (interrupted decoupling) shows nonprotonated aromatic-olefinic carbon from 160 ppm to 120 ppm, and nonprotonated carbon near silicon and methyls (10 ppm to -10 ppm) in the residue. The top spectrum (difference spectrum: normal spectrum minus interrupted decoupling spectrum) shows protonated carbon in the residue.

cause using the concepts known in the polymer blends field, FR polymer formulations can be prepared to yield materials with the same or improved physical properties that are recyclable (because the decomposition temperatures of the pre-ceramics are above the processing temperatures of many polymers) and stable to blooming.

V. SILICATES

Levchik and co-workers recently reported on their investigation of the effect of talc ($3\text{MgO}\cdot 4\text{SiO}_2\cdot \text{H}_2\text{O}$) on the flammability properties of polyamide-6 (PA-6) flame retarded with ammonium polyphosphate (APP) (48). When APP and talc

Table 3 Flammability Properties of PA-6 with APP and Talc Formulations, LOI, and UL-94 Classification

APP/Talc	LOI	UL-94
1:0	25	Nonclassified
10:1	34	Nonclassified
7:1	39	V-2
6:1	42	V-1
3:1	36	V-1
2:1	34	V-0
1:1	27	V-1

Note: All formulations are 80% mass fraction PA-6 and 20% mass fraction of APP or APP and talc.

were combined in a 6:1 ratio (mass ratio), a LOI of 42 resulted. This compares to the talc-free formulation (PA-6, 80% mass fraction, and APP, 20% mass fraction), which gave a LOI of 25. The best UL-94 rating was observed when the APP and talc were combined in a 2:1 ratio (mass ratio). Interestingly, the LOI of this formulation was only 34 (see Table 3). Previously, in PA-6 formulations with less than a 30% mass fraction of APP, they found that although a reaction occurs between the APP and the PA-6 to form a phosphorus oxynitride “char,” the surface char flowed down the sample reexposing the surface to the flame. Furthermore, they proposed that volatilization of phosphoric acid also contributed to a lower LOI.

In a separate study (49) of the thermal behavior of APP and talc, Levchik and co-workers found that the TGA residue yields doubled when the additives were combined, as compared to when they were heated separately. Detailed analysis of x-ray diffraction data showed that these residues were reaction products of talc and APP; for the APP:talc ratio of 2:1, ammonium magnesium polyphosphate, $\text{MgNH}_4(\text{PO}_3)_3$, and ammonium silicon tetrapolyphosphate, $\text{Si}(\text{NH}_4)_2\text{P}_4\text{O}_{13}$, were found to form at 300°C, followed at higher temperature (~400°C) by loss of all nitrogen and the formation of magnesium cyclotetrapolyphosphate, $\text{Mg}_2\text{P}_4\text{O}_{12}$, and silicon oxomonophosphate, $\text{Si}_5\text{O}(\text{PO}_4)_6$. It was proposed by the authors that the talc gave a high-viscosity char due to the presence of the above compounds, which prevented dripping and resulted in a V-0 rating in the UL-94 test. Furthermore, in linear pyrolysis experiments with the PA-6/APP/talc formulations, Camino found that char formed earlier in the presence of talc and that the thermal shielding effect of the char increased with increasing talc content. The formulations with talc formed a less expanded char.

Bourbigot and Le Bras and co-workers have also studied the effect silicates have on the flammability of various polymers. They investigated the effect of a variety of *aluminosilicates* on the performance of intumescent FR formulations

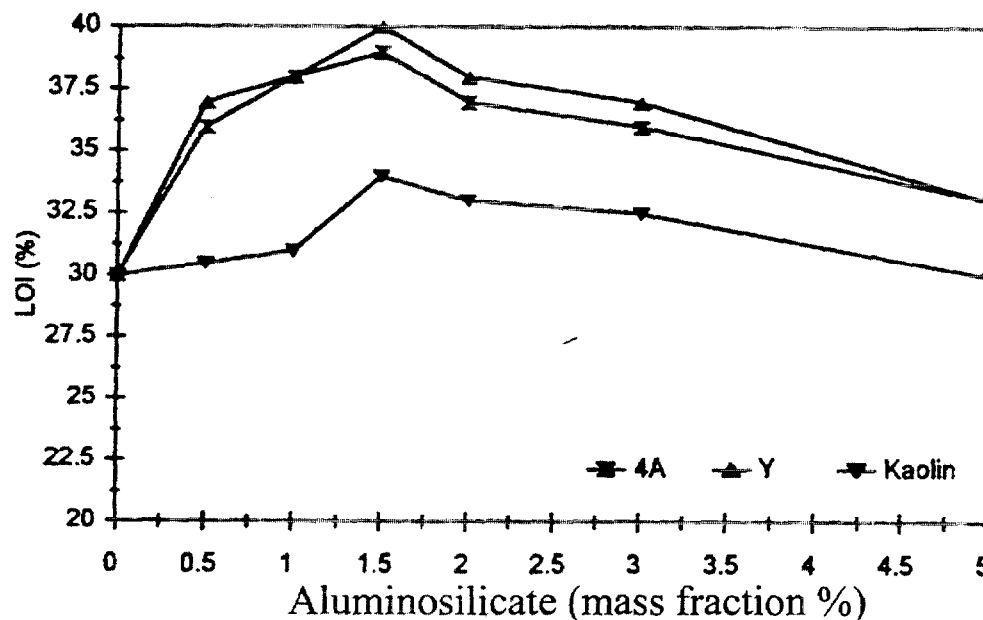


Figure 15 Limiting oxygen index versus 4A-type zeolite, Y-type zeolite and clay (Kaolin) levels in LRAM-3.5, compounded with APP/PER (total additive level remains constant at a mass fraction of 30%). (From Ref. 51.)

(50,51). Zeolites and clays were used in combination with the APP, pentaerythritol (PER) intumescent system. According to Le Bras, clays were originally used in their laboratory as processing aids for increasing the mixing during extrusion and allowing fiber spinning for the manufacture of nonwoven fabrics. Bourbigot credits Beyer et al. with first proposing the use of zeolites to improve FR materials (52).

A comparison of the FR effectiveness of the two types of aluminosilicates in flame-retarding poly(ethylene-butyl acrylate-maleic anhydride) (95:5:3.5 mass ratio of comonomers, respectively) (LRAM-3.5), compounded with APP/PER (total additive level remains constant at a mass fraction of 30%), is shown in Fig. 15. The improvement in FR performance is greater at all loading levels for the zeolites as compared to the clay. For both systems, a mass fraction of 1.5% yields the best results.

Bourbigot and Le Bras carried out an extensive study of the effects of varying the chemical and structural aspects of the zeolites and clays on the flammability performance of the APP/PER FR system. In the zeolite and clay systems, these variations only introduced subtle changes in the LOI at the level where the improvement was best (mass fraction of aluminosilicate = 1.5%). For example, they reported "no relation between the type of exchangeable cation or the aperture size of the zeolites and the FR performance, and that the use of a aluminosilicate with a zeolitic structure (instead of a clay structure) leads to the best FR performance."

A detailed characterization of the pyrolysis residues of 4A-type zeolite with

APP/PER prepared at various temperatures reveals evidence of reaction of the aluminosilicate with APP. A solid-state ^{29}Si -NMR characterization of pyrolysis residues of the additives [APP/PER/4A (Fig. 16)] shows signals (see samples prepared at 350°C and 560°C) at -120 ppm and -215 ppm. These signals are assigned to $[\text{SiO}_4]$ and $[\text{SiO}_6]$ structures, respectively. The chemical shifts of these signals are moved upfield. This provides evidence of phosphorus in the second coordination sphere of Si. These signals are typical for silicophosphate species. Additional evidence of the reaction of the aluminosilicate with the APP was also observed in the MAS ^{27}Al -NMR of the residues. In this case, complete loss of the tetrahedral $[\text{AlO}_4]$ of the zeolite in favor of a new signal characteristic of octahedral $[\text{AlO}_6]$ was observed.

The aluminosilicate reaction with APP is similar to the reaction of APP with talc ($3\text{MgO}\cdot 4\text{SiO}_2\cdot \text{H}_2\text{O}$) observed by Camino and Levchik, as discussed earlier. In both cases, metalophosphate and silicophosphate species are formed, which presumably are responsible for the improvements in flammability observed.

Bourbigot et al. studied the effect of the thermoplastic comonomer composition on the FR performance of the APP/PER/4A system (53). They found that polar comonomers increased the LOI for both the APP/PER formulations and the APP/PER/4A formulations; however, the improvements were 5–30% larger in the latter case. The copolymer that yielded the greatest LOI increase in the presence of the 4A zeolite was LRAM-3.5 [poly(ethylene–butyl acrylate–maleic anhydride) (95:5:3.5 mass ratio of comonomers, respectively)]. Bourbigot et al. proposed that acid functionality from hydrolysis of maleic anhydride or from thermal decomposition of butyl acrylate increased the interaction between the zeolite and the copolymer in the condensed phase during decomposition.

The rate of heat release (RHR) data from Cone calorimetry of the LRAM-3.5, LRAM-3.5–APP/PER, and LRAM-3.5–APP/PER/4A systems is shown in Fig. 17. The peak RHR for each of the two flame-retarded LRAM-3.5 samples is significantly lower than that for the pure LRAM-3.5. Although there is little difference in the *peak* RHRs for the two FR samples, the *average* RHR of the LRAM-3.5–APP/PER/4A sample is $\sim 50\%$ lower than that for the LRAM-3.5–APP/PER sample. According to Bourbigot et al., this difference may be due to the presence of the zeolite and the subsequent reaction during burning with APP to form aluminophosphates and silicophosphates, which leads to a lower fuel feed rate and/or to a different fuel composition.

Although the above systems effectively reduce the flammability of the polymers they are used with, they employ inorganic additives, which have poor compatibility with their host polymers, and therefore degrade the mechanical properties of the formulated product. For example, Bourbigot et al. reports that EVA has a 35% lower elongation at break, when formulated with a mass fraction of 30% silane-treated aluminium trihydrate (ATH) (54). For the purpose of improving the mechanical properties and FR performance of these systems, the above research groups continue their work.

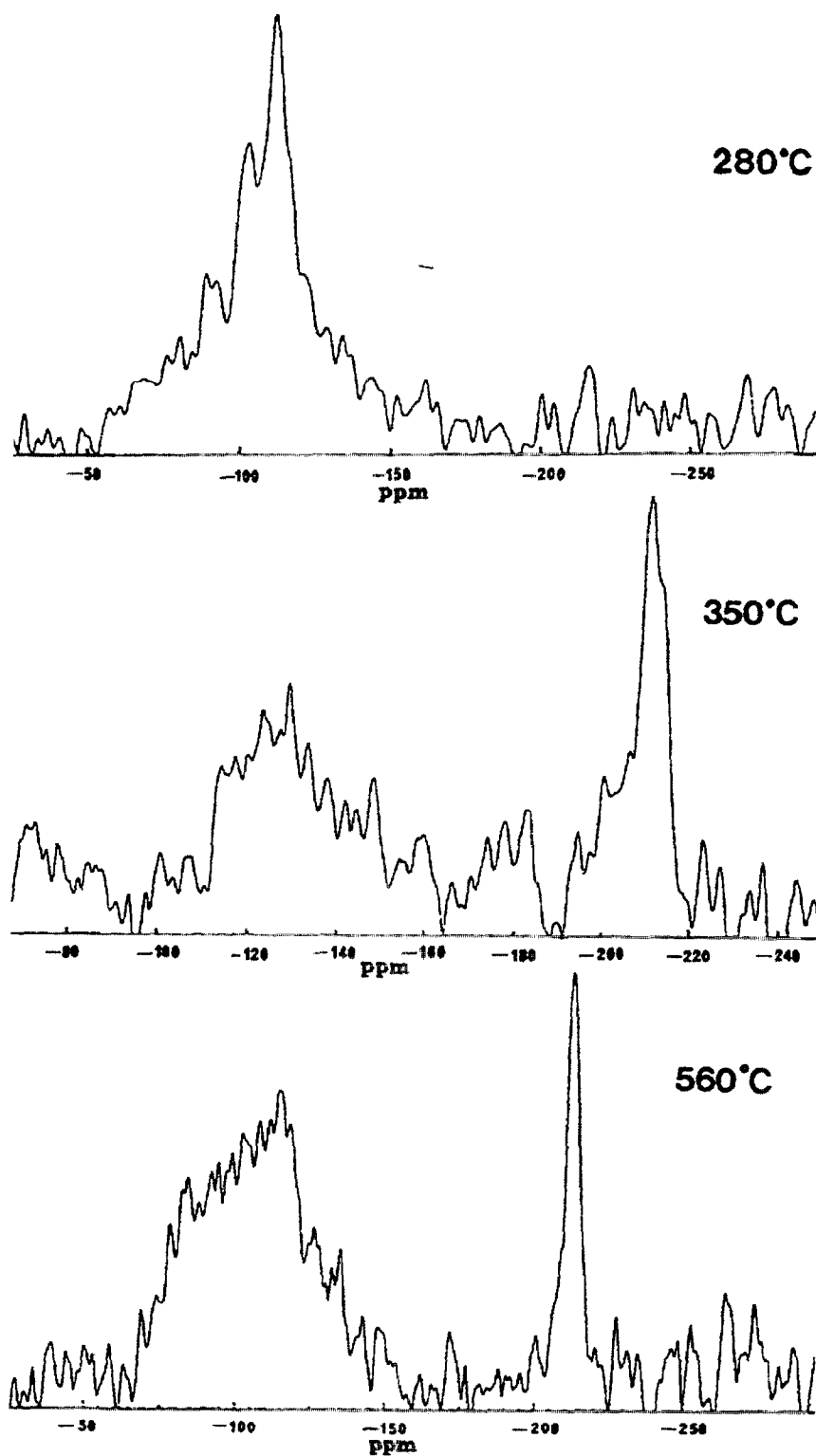


Figure 16 MAS ^{29}Si NMR Si-spectra of pyrolyzed APP/PER/4A. (From Ref. 53.)

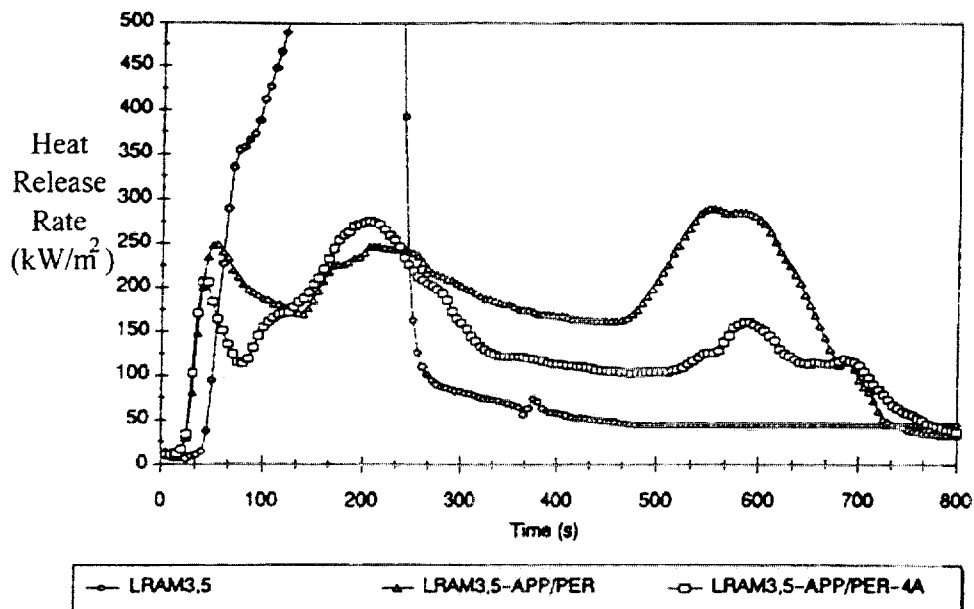


Figure 17 Rate of heat release versus time for the LRAM-3.5, LRAM-3.5-APP/PER, and LRAM-3.5-APP/PER/4A zeolite samples (95:5:3.5 mass ratio of comonomers, respectively) (LRAM-3.5), samples compounded with APP/PER (total additives level remains constant at mass fraction of 30%, mass fraction of aluminosilicate 1.5%). (From Ref. 53.)

Two other groups, Wilkie et al. and Corbin et al. have also used zeolites as flame retardants. Wilkie and co-workers has used zeolites as Friedel-Crafts catalysts for cross-linking benzene dimethanol with polystyrene at temperatures above 300°C in a sealed tube (55,56). Unfortunately, this reaction does not occur in an open system, due to volatilization of the diol. However, Wilkie and co-workers found that hydroxyalkyl-substituted copolymers will cross-link in an open system (57). Corbin et al. in a recent Patent Cooperation Treaty application showed how the use of various zeolites at low loading levels (mass fraction of 2–5%) produced UL-94 V-0 ratings in formulations of fiber-reinforced thermotropic liquid-crystalline polymers (LCP) (58).

VI. POLYMER LAYERED-SILICATE (CLAY) NANOCOMPOSITES

Recently, Gilman, et al. reported on the promising flammability properties of polymer layered-silicate (clay) nanocomposites (59). Polymer clay nanocomposites are hybrid organic polymer-inorganic materials that consist of alternating, nanometer-thick layers of polymer and mica-type silicate.

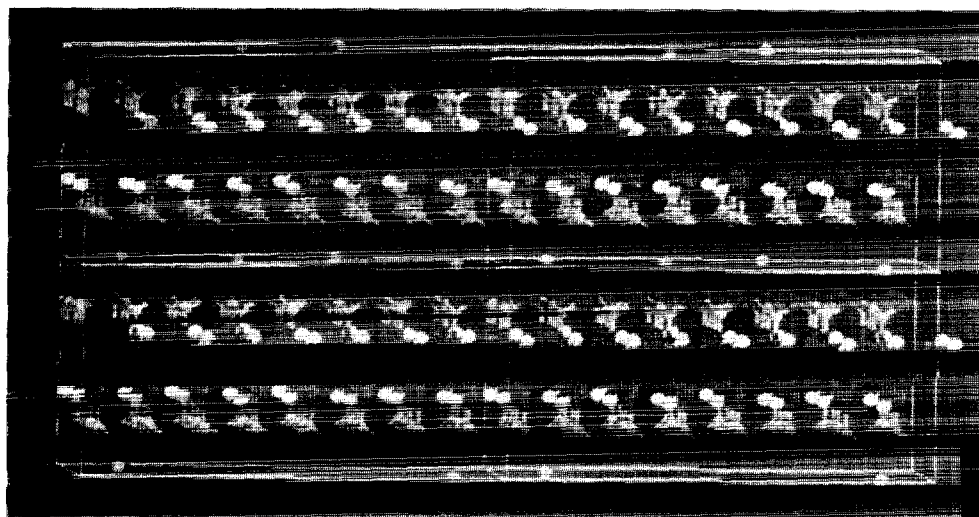


Figure 18 Molecular representation of sodium montmorillonite, showing two aluminosilicate layers with the Na^+ cations in the interlayer gap or gallery (1.14 nm layer-to-layer spacing).

The most recent methods of preparing polymer clay nanocomposites have been developed by several groups during the last decade (60–66). In general, these methods achieve molecular-level incorporation of the layered silicate (e.g., montmorillonite) into the polymer by the addition of a modified silicate; either during the polymerization (*in situ* method), or to a solvent-swollen polymer, or to the polymer melt (67).

Two terms (*intercalated* and *delaminated*) are used to describe the two general classes of nanomorphology that can be prepared. *Intercalated* structures are well-ordered multilayered structures, where only a one or two layers of extended polymer chains are inserted into the gallery space between the individual silicate layers (see Fig. 18). The *delaminated* (or *exfoliated*) structures result when the individual silicate layers are well dispersed in the organic polymer. The interlayer spacing (2–200 nm) is on the order of the radius of gyration of the polymer. The silicate layers in a *delaminated* structure may not be as well ordered as in an *intercalated* structure and are also referred to as *exfoliated* or *disordered* nanocomposites. Tan and Pinnavaia has presented a rigorous definition of these terms (66).

Polymer clay nanocomposites have unique properties when compared to conventional filled polymers (67). For example, the mechanical properties of a nylon 6 mica-type layered-silicate nanocomposite, with a silicate mass fraction of only 5%, show excellent improvement over those for the pure nylon 6. The nanocomposite exhibits a 40% higher tensile strength, 68% greater tensile modulus, 60% higher flexural strength, and a 126% increased flexural modulus. The heat

distortion temperature (HDT) is increased from 65°C to 152°C (63) and the impact strengths are only lowered by 10%. Some nanocomposites exhibit increased thermal stability—an important property for improving flammability performance. Furthermore, decreased gas permeability and increased solvent resistance accompany the improved physical properties.

In 1965, Blumstein first reported the improved thermal stability of a polymer clay nanocomposite that combined PMMA and montmorillonite clay (68). Blumstein found the PMMA inserted between the lamellae of montmorillonite clay resisted thermal degradation under conditions that completely degraded pure PMMA. The first mention of the potential FR properties of this type of material appears in a 1976 Japanese patent application on nylon 6 nanocomposites (69). However, not until Gianellis and co-workers reported self-extinguishing behavior in a polyimide clay nanocomposite did the serious evaluation of the unique flammability properties of these materials begin (64). Characterization of the flammability properties of a variety of polymer clay nanocomposites, by Gilman et al. revealed that this approach results in lower flammability for many different types of polymers (59,70).

Gilman reported on the flammability properties of several *thermoplastic* polymer nanocomposites; *delaminated* nylon 6 layered-silicate nanocomposites and *intercalated* nanocomposites prepared from PS and PP. The flammability data for nylon 6, nylon 12, PS, and PP is shown in Table 4. The Cone Calorimetry data shows that both the peak and average heat release rates (HRR) were reduced significantly for *intercalated* and *delaminated* nanocomposites with low silicate mass fraction (2–5%). Similar results were also reported for thermoset polymer nanocomposites made from vinyl esters and epoxies (71). The HRR plots for nylon 6 and nylon 6 silicate nanocomposites (mass fraction 5%) at 35 kW/m² heat flux are shown in Fig. 19 and are typical of those found for all the nanocomposites in Table 4. The nylon 6 nanocomposite has a 63% lower HRR than the pure nylon 6. Furthermore, for the PS silicate nanocomposite, the magnitude of improvement in flammability performance is comparable to that found for PS flame retarded using a total mass fraction of 30% of decabromodiphenyl oxide (DBDPO) and antimony trioxide (Sb₂O₃) (see Table 4). This is accomplished without as much of an increase in the soot (SEA) or CO yields. The data also indicate that the rate of mass loss during combustion of the nanocomposite is significantly reduced from the values observed for the pure polymers (see Fig. 20). The heat of combustion, SEA, and carbon monoxide yields are unchanged; this suggests that the source of the improved flammability properties of these materials is due to differences in condensed-phase decomposition processes and not to a gas-phase effect.

A comparison of the residue yields for the nanocomposites in Table 4 reveals little improvement in the carbonaceous char yields, once the presence of the

Table 4 Cone Calorimeter Data

Sample (structure)	Residue yield (%) ±0.5	Peak HRR ($\Delta\%$) (kW/m ²)	Mean HRR ($\Delta\%$) (kW/m ²)	Mean H_c (MJ/kg)	Mean SEA (m ² /kg)	Mean CO yield (kg/kg)
Nylon 6	1	1010	603	27	197	0.01
Nylon 6 silicate nanocomposite 2% (delaminated)	3	686 (32%)	390 (35%)	27	271	0.01
Nylon 6 silicate nanocomposite 5% (delaminated)	6	378 (63%)	304 (50%)	27	296	0.02
Nylon 12	0	1710	846	40	387	0.02
Nylon 12 silicate nanocomposite 2% (delaminated)	2	1060 (38%)	719 (15%)	40	435	0.02
PS	0	1120	703	29	1460	0.09
PS silicate mix 3% (immiscible)	3	1080	715	29	1840	0.09
PS silicate nanocomposite 3% (intercalated)	4	567 (48%)	444 (38%)	27	1730	0.08
PS w/DBDPO/ SB ₂ O ₃ 30%	3	491 (56%)	318 (54%)	11	2580	0.14
PP	0	1525	536	39	704	0.02
PP silicate nanocomposite 2% (intercalated)	5	450 (70%)	322 (40%)	44	1028	0.02

Heat flux: 35 kW/m², H_c : Heat of combustion. SEA: Specific Extinction Area. Peak heat release rate, mass loss rate and specific extinction area (SEA) data, measured at 35 kW/m², are reproducible to within ±10%. The carbon monoxide and heat of combustion data are reproducible to within ±15%.

silicate in the residue is taken into account. These data indicate that the mechanism of flame retardancy may be very similar for each of the systems studied and that the lower flammability is not due to retention of a large fraction of carbonaceous char in the condensed phase. This is in contrast to other studies of the pyrolysis reactions of organic compounds in layered-silicate intercalates. These studies reported formation of carbonaceous silicate residues and other condensation and cross-linking-type reaction products (72). Additional support for a common FR mechanism comes from studies of the condensed-phase pyrolysis processes, us-

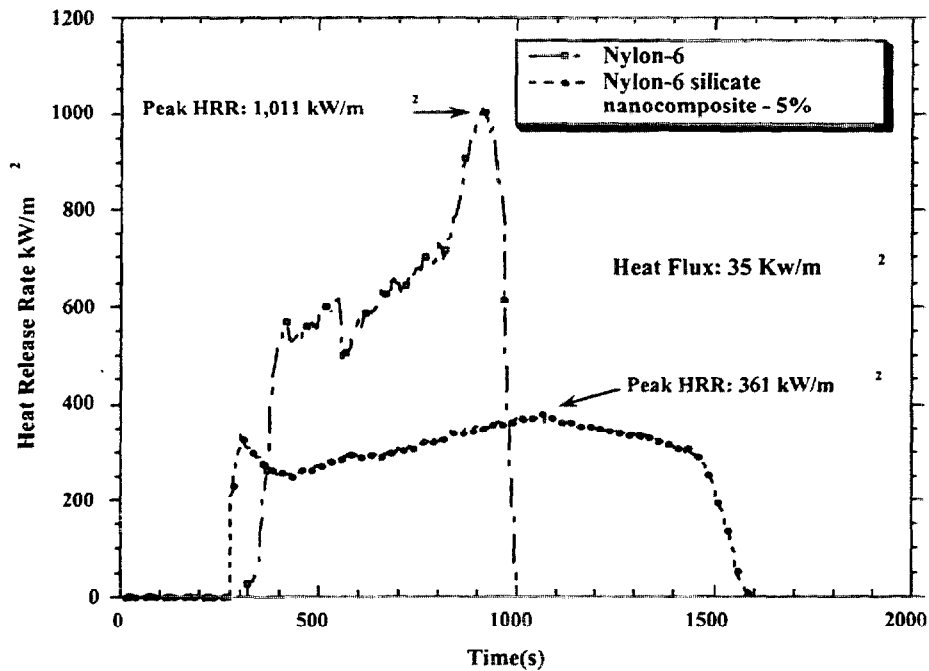


Figure 19 Comparison of the HRR plot for nylon 6 and nylon 6 silicate nanocomposites (mass fraction 5%) at 35 kW/m² heat flux, showing a 63% reduction in HRR for the nanocomposite.

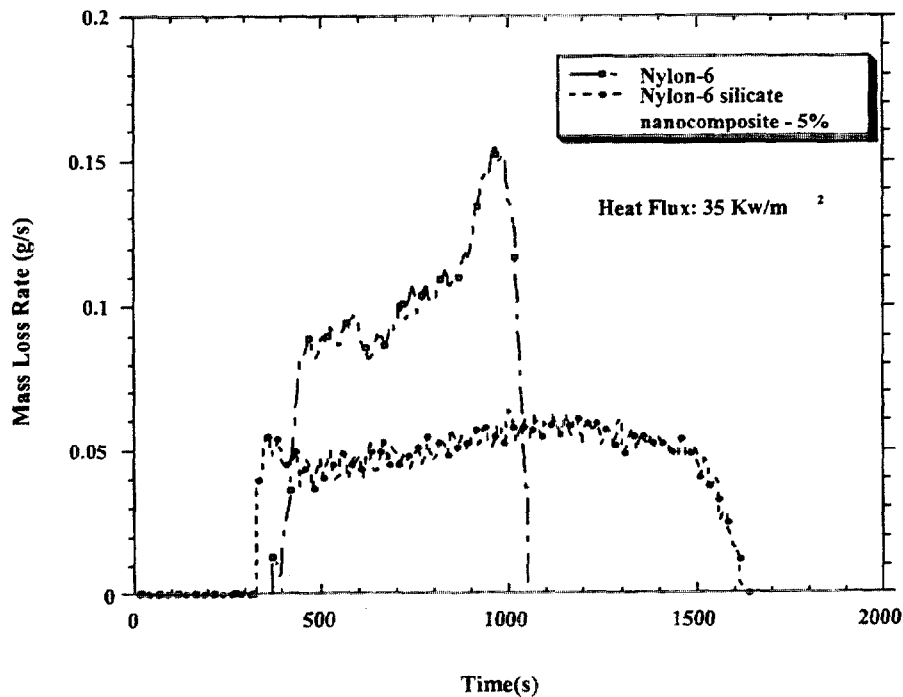


Figure 20 The mass loss rate data for nylon 6 and nylon 6 silicate nanocomposites (5%). The curves closely resemble the HRR curves (Fig. 19), indicating that the reduction in HRR for the nanocomposites is primarily due to the reduced mass loss rate and the resulting lower fuel feed rate to the gas phase.

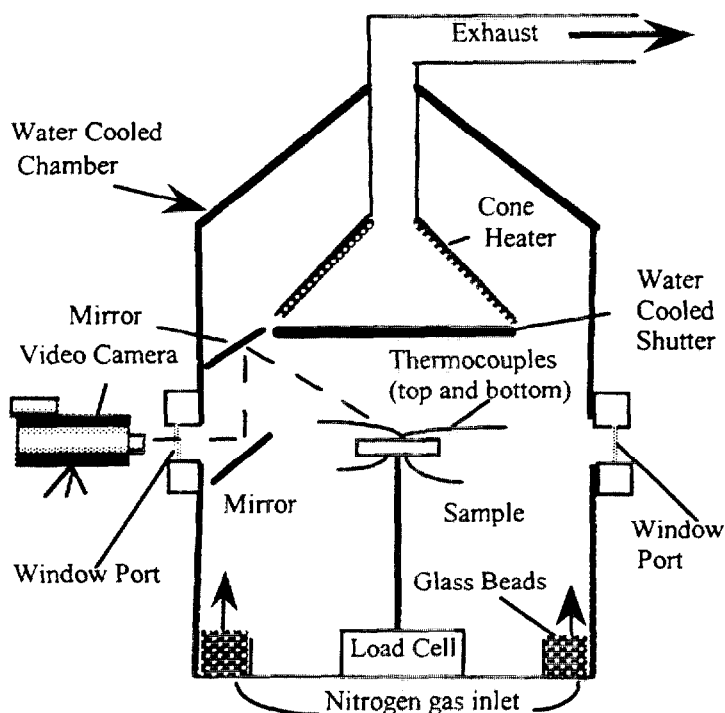


Figure 21 A schematic of the radiative gasification apparatus (diameter = 0.6 m, height = 1.7 m). The gasification apparatus allows pyrolysis, in a nitrogen atmosphere, of samples identical to those used in the Cone Calorimeter.

ing the radiative gasification device shown in Fig. 21. X-ray diffraction (XRD) and transmission electron microscopy (TEM) analysis of the combustion chars from a variety of nanocomposites were also performed.

The mass loss rate (MLR) data for nylon 6 and nylon 6 clay nanocomposites, gathered in the N_2 gasification apparatus, are shown in Fig. 22. Visual observation of the pyrolysis shows that at 180 s, when the MLR for the nylon 6 silicate nanocomposite slows compared to the pure nylon 6, char covers over 50% of the sample's surface.

The TEM of a section of the combustion char from the nylon 6 silicate nanocomposite (5%) is shown in Fig. 23. A multilayered silicate structure is seen after combustion, with the darker, 1-nm-thick silicate sheets forming a large array of fairly even layers. This was the primary morphology seen in the TEM of the char; however, some voids were also present. The delaminated hybrid structure appears to collapse during combustion. The nanocomposite structure present in the resulting char appears to enhance the performance of the char through reinforcement of the char layer. This multilayered silicate structure may act as an excellent insulator and mass-transport barrier, slowing the escape of the volatile

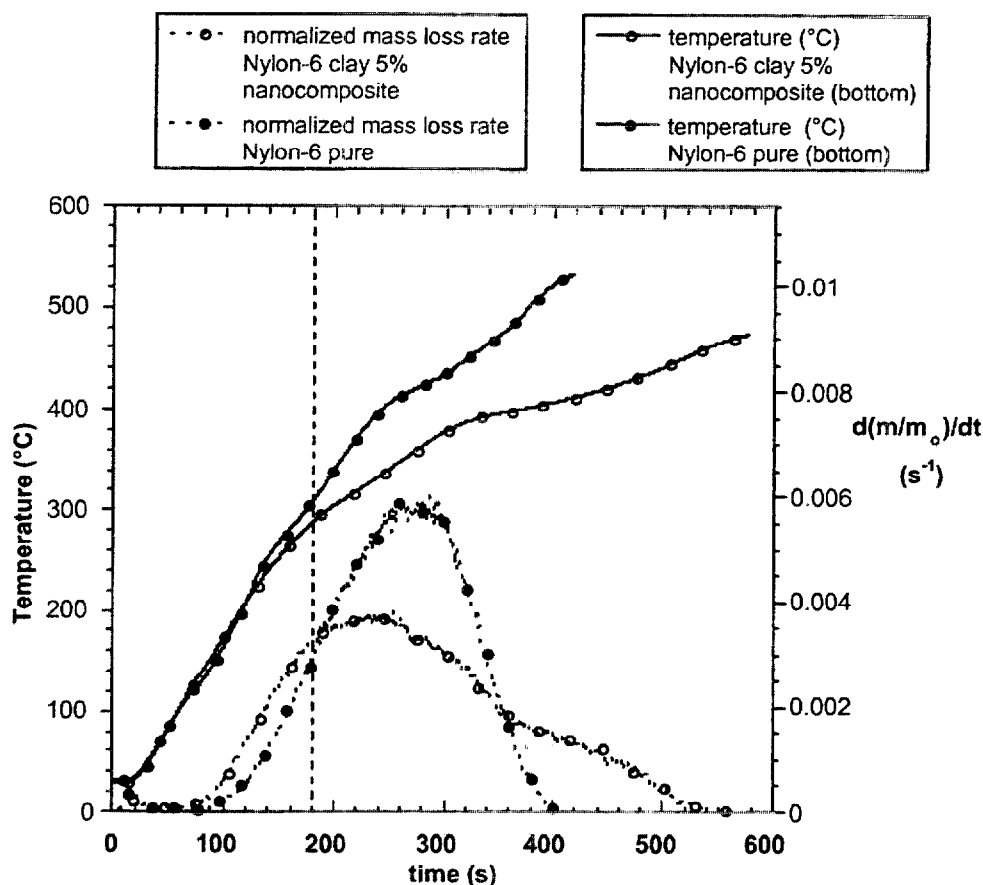


Figure 22 Normalized mass loss rate and temperature versus time plots for the gasification experiments for nylon 6 and nylon 6 silicate (5%) nanocomposites in a N_2 atmosphere. All samples were exposed to a flux of 40 kW/m^2 in a N_2 atmosphere. The mass loss rate curves begin to differ at 180 s when the surface of the nanocomposite sample is partially covered by char. The insulating effect of the char can be seen in the bottom-surface thermocouple data for the nanocomposite.

products generated as the nylon 6 decomposes (70). Analysis of combustion chars, by XRD, from nylon 6 and epoxy nanocomposites shows that the interlayer spacing of all three chars is 1.3 nm. This result is independent of the chemical structure (*thermoplastic* polyamide, *thermosetting* aromatic amine-cured epoxy or tertiary amine-cured epoxy), or nanostructure (*delaminated* or *intercalated*) of the original nanocomposite (70).

Polymer clay nanocomposites are materials that may fulfill the requirements for a high-performance, additive-type flame-retardant system (i.e., one that reduces flammability while improving, or at least not drastically degrading, the other performance properties of the final formulated product). Indeed, a 1998 Jap-

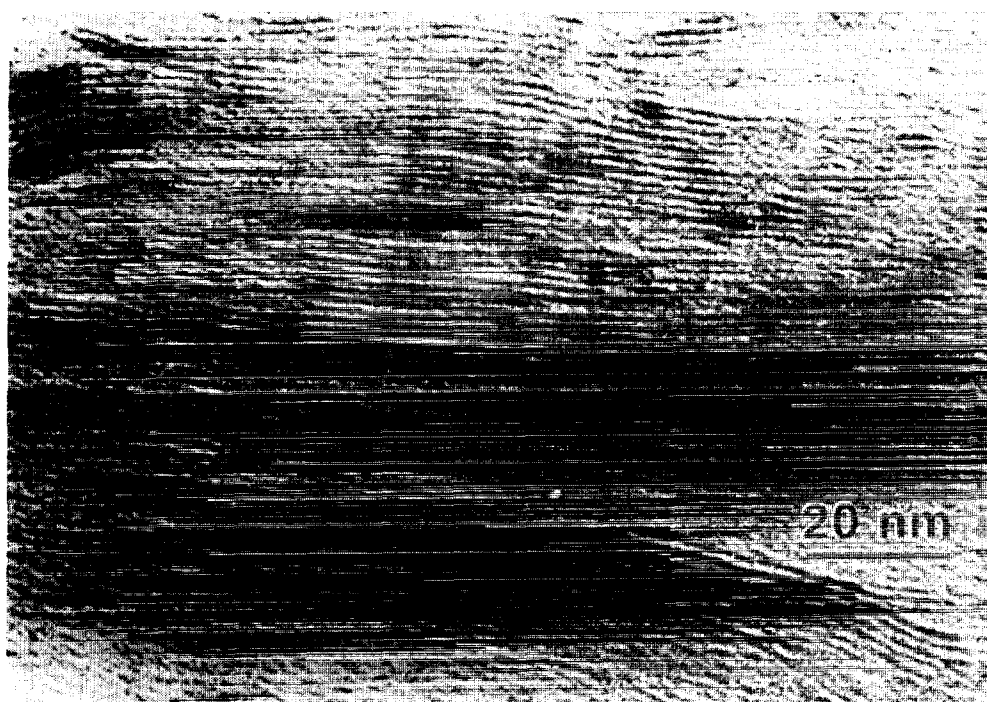


Figure 23 TEM of a section of the combustion char from the nylon 6 silicate nanocomposite (5%) showing the carbon silicate (1 nm thick, dark bands) multilayered structure. This layer may act as an insulator and a mass-transport barrier.

anese patent by Inoue and Hosokawa teaches the use of “silicate-triazine intercalation compounds in fire resistant polymeric composites” (73). By combining the known FR properties of melamine and those of polymer clay nanocomposites, the inventors produced V-0 ratings in the UL-94 flammability test while increasing both the bending modulus and the heat distortion temperature. Nylon 6, poly(butylene phthalate) (PBT), poly(oxymethylene) (POM), and polyphenylene sulfide (PPS) were prepared as silicate-triazine nanocomposites using the synthetic silicate fluorohectorite. Various melamine salts were intercalated into the clay; 10–15% total mass fraction of modified clays were used along with additional melamine (mass fraction 5%). Inoue and Hosokawa characterized the spacing between the clay layers using TEM; they found that without a uniform dispersion of the clay layers in the polymer only a Horizontal Burn (HB) rating was obtained (73).

VII. SUMMARY

This chapter has presented an overview of silicon-based flame retardants. It is apparent that considerable resources are being focused on this new area both to develop new products and to develop a better understanding of the flame-retardant

mechanisms. In general, a condensed-phase mechanism which involves a silicon-based protective surface layer is proposed. Most of these systems do not enhance formation of carbonaceous char. Thus, we propose that there exists a subset FR mechanism within the general class of "char-enhancing flame retardants" in which high-performance char barrier forms. This high-performance char acts as an insulator and mass-transport barrier, but does not retain additional carbon in the condensed phase. Indeed, this is an advantage for this type of fire retardant, because many countries are now recycling via pyrolysis processes, which cause depolymerization and yield useful hydrocarbon feedstocks. Several of these approaches not only offer improved flammability performance but also provide the added benefit of improved physical properties and recyclability.

REFERENCES

1. S Serizawa, M Iji. European Patent EP 829521 A1 980318, 1998.
2. Y Ueda, K Furukawa. Jpn Kokai Tokkyo Koho, JP 09183870 A2 970715, 1997.
3. DH Blount. US Patent 5563285 A 961008, 1996.
4. ED Weil, W Zhu. PCT Int. Appl. WO 9510565 A2 950420, 1995.
5. A Nishio, H Ogawa. Jpn Kokai Tokkyo Koho, JP 05194876 A2 930803, 1994.
6. LL Musselman, LF Wieserman. US Patent 4781982 A 881101, 1989.
7. M Iji, S Serizawa. *Poym Adv Technol* 9:593–600, 1998.
8. RP Kambour, JE Corn, S Miller, GE Niznik. *J Appl Polym Sci* 20:3275–3293, 1976.
9. RP Kambour, WV Ligon, RP Russell. *J Polym Sci Polym Lett Ed* 16:327–333, 1978.
10. A Factor, KN Sannes, AM Colley. *J Fire Flamm* 12:101–107, 1981.
11. RP Kambour, HJ Klopper, SA Smith. Limiting oxygen indices of silicone block polymers. *J Appl Polym Sci* 26:847–859, 1981.
12. RP Kambour. *J Appl Polym Sci* 26:861–877, 1981.
13. DR Olson. Proceeding of the Fifteenth International Conference on Fire Safety, 1990, pp. 328–336.
14. R Benrashid, GL Nelson. In: GL Nelson, ed. *Fire and Polymers II*. ACS Symposium Series 599. Washington, DC: American Chemical Society, 1995, pp. 217–235.
15. DW Van Krevelen. *Polymer* 16:615–620, 1975.
16. T Kashiwagi, TG Cleary, GC Davis, JH Lupinski. Proceedings of International Conference for the Promotion of Advanced Fire Resistant Aircraft Interior Materials, DOT/FAA/CT-93/3, 1993, pp. 175–187.
17. JR Ebdon, JB Hunt, MS Jones, FG Thorpe. *Polym Degrad Stabil* 54:395–400, 1996.
18. GE Zaikov, SM Lomakin. *Polym News* 20:289–291, 1995.
19. GE Zaikov, SM Lomakin. *Polym Degrad Stabil* 54:223–233, 1996.
20. KR Hartley, DL Finney, RB Bush. International Wire & Cable Symposium Proceedings, 1986, pp. 567–574.
21. RB Bush. *Plastics Eng* 43:29–32, April 1986.
22. BR Frye. In: DR Paul, LH Sperling, eds. *Multicomponent Polymer Materials*. Advances in Chemistry Series 211. Washington, DC: American Chemical Society, 1986, pp. 337–342.

23. JE Hirvensalo, JE Robinson, T Smith, OA Wiklund. In: 4th International Conference and Exhibition. London: Interscience Communications, 1995, pp. 245–254.
24. W Gardiner, R Buch, D Romenesko. In: INTERFLAM 93. London: Interscience Communications, 1993, pp. 675–687.
25. MR MacLaury, AL Schroll. *J Appl Polym Sci* 30:461–472, 1985.
26. PK Huester. *J Cell Plastic* 10:186–193, July/August 1974.
27. B Prokai, PK Huester, B Kanner. In: VM Bhatnagar, ed., Proceedings of 1975 International Symposium on Flammability and Fire Resistance. Technomic Publication, Westport, Conn., 1975, pp. 264–281.
28. NS Allen, M Edge, T Corrales, A Childs, C Liauw, F Catalina, C Peinado, A Minihan. *Polym Degrad Stabil* 56:125–139, 1997.
29. MR MacLaury. *J Fire Flamm* 10:175–198, 1979.
30. G Bertelli, G Camino, E Marchetti, L Costa, E Casorati, R Locatelli. *Polym Degrad Stabil* 25:277–292, 1989.
31. Gy Marosi, P Anna, I Balogh, Gy Bertalan, A Tohl, MA Maatoug. *J Therm Anal* 48:717–726, 1997.
32. PJ Austin, RR Buch, T Kashiwagi. *Fire Mater* 22:221–237, 1998.
33. S Heidari, R Kallonen. *Fire Mater* 17:21–24, 1993.
34. JW Gilman, SJ Ritchie, T Kashiwagi, SM Lomakin. *Fire Mater* 21:23–32, 1997.
35. ML Hoppe, RM Laine, J Kampf, MS Gordon, LW Burggraf. *Angew Chem Int Ed Engl* 32:287–289, 1993.
36. CF Cullis, AC Norris. *Carbon* 9:517–520, 1971.
37. RK Iler. *The Chemistry of Silica*. New York: Wiley, 1979, pp. 588–591.
38. CAB-O-SIL Untreated Fumed Silica Properties and Functions, Cabot Corp., Tuscola, IL, TD-100, May 1997.
39. F-U Hshieh. *Fire Mater* 22:69–76, 1998.
40. J Lichtenhan, J Gilman. *US Patent Appl.*, May 28, 1997.
41. JW Gilman, T Kashiwagi, RH Harris Jr, S Lomakin, JD Lichtenhan, P Jones, A Bolf. In: S Al-Malaika, C Wilkie, CA Golovoy, eds. *Chemistry and Technology of Polymer Additives*. London: Blackwell Science, 1999, pp. 135–150.
42. W Kowbel, R Viadyanathan, JR Patel, JC Withers. Proceedings of 43rd International SAMPE Symposium, Anaheim, 1998, pp. 1018–1028.
43. TC Chao, SK Sarmah, RP Boisvert, GT Burns, DE Katsoulis, WC Page. Proceedings of 43rd International SAMPE Symposium, Anaheim, 1998, pp. 1029–1041.
44. AG Bolf, JD Lichtenhan. *Am Chem Soc Polym Prepr* 35:527–528, 1994.
45. V Babrauskas, RD Peacock. *Fire Safety J* 18:255, 1992.
46. J Gilman, S Ritchie, T Kashiwagi, S Lomakin, D VanderHart, V Nagy. *Fire Mater* 22:61–67, 1998.
47. JS Hartman, MF Richardson, BL Sherriff, BG Winsborrow. *J Am Chem Soc* 109:6059–6067, 1987.
48. SV Levchik, GF Levchik, G Camino, L Costa. *J Fire Sci* 13:43–58, 1995.
49. GF Levchik, AF Selevich, SV Levchik, AI Lesnikovich. *Thermochim Acta Thermal Behavior of Ammonium Polyphosphate-Inorganic Compound Mixtures. Part I. Talc.* 239:41–49, 1994, and patent references cited therein.
50. S Bourbigot, M Le Bras, P Breant, JM Tremillon, R Delobel. *Fire Mater* 20:145–154, 1996.

51. M Le Bras, S Bourbigot. *Fire Mater* 20:39–49, 1996.
52. HK Beyer, G Borbely, P Miasnikov, P Rozsa. In: HG Karge, J Weitkamp, eds. *Zeolites as Catalysts, Sorbents and Detergent Builders*. Amsterdam: Elsevier, 1985, p. 635.
53. S Bourbigot, M Le Bras, P Breant, JM Tremillon. *Polym Degrad Stabil* 54:275–287, 1996.
54. S Bourbigot, M Le Bras, F Dabrowski, J Gilman, T Kashiwagi. *Proceedings of 10th BCC Annual Conference*, Stamford, CT, 1999, pp. 1–21.
55. J Li, CA Wilkie. *Polym Degrad Stabil* 57:293–299, 1997.
56. Z Wang, DD Jiang, MA McKinney, CA Wilkie. *Polym Degrad Stabil* (in press).
57. Z Wang, DD Jaing, CA Wilkie, JW Gilman. *Polym Degrad Stabil* (in press).
58. DR Corbin, SG Cottis, IG Plotzker. *PCT Int. Appl. WO 98/28380*, July 2, 1998 (to E. I. Dupont de Nemours and Co., USA).
59. J Gilman, T Kashiwagi, J Lichtenhan. *SAMPE J* 33:40–46, 1997.
60. MS Wang, TJ Pinnavaia. *Chem Mater* 6:468–474, 1994.
61. A Usuki, M Kato, A Okada, T Kurauchi. *J Appl Polym Sci* 63:137–139, 1997.
62. A Usuki, Y Kojima, M Kawasumi, A Okada, Y Fukushima, T Kurauchi, O Kamigaito. *J Mater Res* 8:1179–1184, 1993.
63. Y Kojima, A Usuki, M Kawasumi, A Okada, Y Fukushima, T Kurauchi, O Kamigaito. *J Mater Res* 8:1185–1189, 1993.
64. J Lee, T Takekoshi, E Giannelis. *Mater Res Soc Symp Proc* 457:513–518, 1997.
65. J Lee, E Giannelis. *Am Chem Soc Polym Prepr* 38:688–689, 1997.
66. L Tan, TJ Pinnavaia. *Mater Res Soc Symp Proc* 435:79–84, 1996.
67. EP Giannelis. *Adv Mater* 8:29–35, 1996.
68. A Blumstein. *J Polym Sci Part A* 3:2665–2672, 1965.
69. S Fujiwara, T Sakamoto. *Kokai Patent Appl. SHO 51(1976)-109998*, September 1976.
70. JW Gilman, T Kashiwagi, S Lomakin, EP Giannelis, E Manias, JD Lichtenhan, P Jones. In: G Camino, M Le Bras, S Bourbigot, R DeLobel, eds. *Fire Retardancy of Polymers: The Use of Intumescence*. Cambridge: The Royal Society of Chemistry, 1998, pp. 203–221.
71. JW Gilman, T Kashiwagi, M Nyden, JET Brown, CL Jackson, S Lomakin, EP Giannelis, E Manias. In: S Al-Malaika, C Wilkie, CA Golovoy, eds. *Chemistry and Technology of Polymer Additives*. London: Blackwell Science, 1999, pp. 249–265.
72. JM Thomas. *Intercalation Chemistry*. London: Academic Press, 1982, pp. 79–81.
73. H Inoue, T Hosokawa. *Japan Patent. Jpn Kokai Tokkyo Koho JP 10 81,510 (98 81,510)* (to Showa Denko K. K. Japan).

